Contents lists available at ScienceDirect

Deep-Sea Research Part I

Interaction between active tectonics, bottom-current processes and coral mounds: A unique example in the NW Moroccan Margin, southern Gulf of Cadiz

Débora Duarte [a,b,c,*], Vitor Hugo Magalhães [b,d], F. Javier Hernández-Molina [a,e], Cristina Roque [d,f], Walter Menapace [g,h]

[a] *Dept. Earth Sciences, Royal Holloway Univ. London, Egham, Surrey, TW20 0EX, UK*
[b] *Divisão de Geologia e Georecursos Marinhos, Instituto Português do Mar e da Atmosfera – IPMA, Lisbon, Portugal*
[c] *The Lyell Centre & EGIS, Heriot-Watt University, Research Avenue South, Edinburgh EH14 4AP, UK*
[d] *Instituto Dom Luiz, Faculty of Sciences, University of Lisbon, Portugal*
[e] *Andalusian Earth Sciences Institute (IACT), Spanish Research Council (CSIC), Granada, Spain*
[f] *Estrutura de Missão de Extensão da Plataforma Continental – EMEPC, Paço d'Arcos, Portugal*
[g] *MARUM – Center for Marine Environmental Sciences, University of Bremen, Germany*
[h] *Institute of Marine Sciences (ICM-CSIC), Department of Marine Geosciences, Barcelona, Spain*

ARTICLE INFO

ABSTRACT

The NW Moroccan Margin has a complex geological evolution, being located close to the transition zone between the Azores – Gibraltar Fracture Zone and the western front of the Betic–Rif collisional orogen. The interaction between tectonic, halokinetic and fluid flow processes with bottom-current activity shapes the seafloor and influences the distribution of seafloor biological communities (such as the cold-water coral mounds) and deep-water sedimentation. The aims of this work are to study the interaction of the paleo-oceanographic and morpho-tectonic processes that generated the various seafloor features of the NW Moroccan Margin. To achieve this, high-resolution multibeam bathymetry and parasound data acquired in the "ALBOCA II" cruise have been used, complemented by high-resolution 2D seismic reflection data and the EMODnet bathymetric compilation.

Several morphological features were identified in the margin, which are related to different processes of sedimentary (contourites and sediment waves), structural (faults and diapirs), gravitational (slide scars, mass transport deposits), fluid migration (mud volcanoes and pockmarks) and biogenic (exposed and buried coral mounds) nature. The structural features (e.g., strike-slip faults) have a major control on the seafloor morphology and, consequently, on the development and evolution of the sedimentary systems in the study area.

The evolution of the NW Moroccan Margin during the late Quaternary has been controlled by climatic variations and tectonic activity. The action of these factors has been dominant in distinct parts of the study area where: *i)* contourite terraces developed when climatic and oceanographic changes were the prevalent factor, *ii)* mounded and confined contourite drifts and local mass transport deposits formed when the major control was tectonic activity.

1. Introduction

Seafloor morphology is shaped by the interaction of several processes, such as tectonic forces, sediment input, climate and sea-level changes, and oceanographic circulation (Artoni et al., 2007; Leeder, 2011; Duarte et al., 2022). In deep-water settings, oceanic circulation is comprised by semi-permanent density-driven currents, known as bottom-currents (Rebesco et al., 2014 and references therein). These currents tend to flow parallel to the continental margin slope (along-slope circulation), but its pathways can be locally modified by topographic structures on the seafloor such as structural highs, fault scarps, seamounts, coral mounds and mud volcanoes (Vandorpe et al., 2014, 2016; Liu et al., 2019, 2021; Duarte et al., 2022).

The Gulf of Cadiz is located to the west of the Strait of Gibraltar,

enclosed by the southwestern Iberian and the northwestern Moroccan margins (Fig. 1a). It corresponds to the transition zone between the Azores – Gibraltar Fracture Zone and the western front of the Betic–Rif collisional orogen (Medialdea et al., 2009; Zitellini et al., 2009; Vergés and Fernàndez, 2012; Terrinha et al., 2019; Ramos et al., 2020). The seafloor morphology is influenced by this setting, with a set of WNW-ESE trending dextral strike-slip faults (i.e., the SWIM faults, Rosas et al., 2009; Terrinha et al., 2009; Zitellini et al., 2009, Fig. 1a and b),
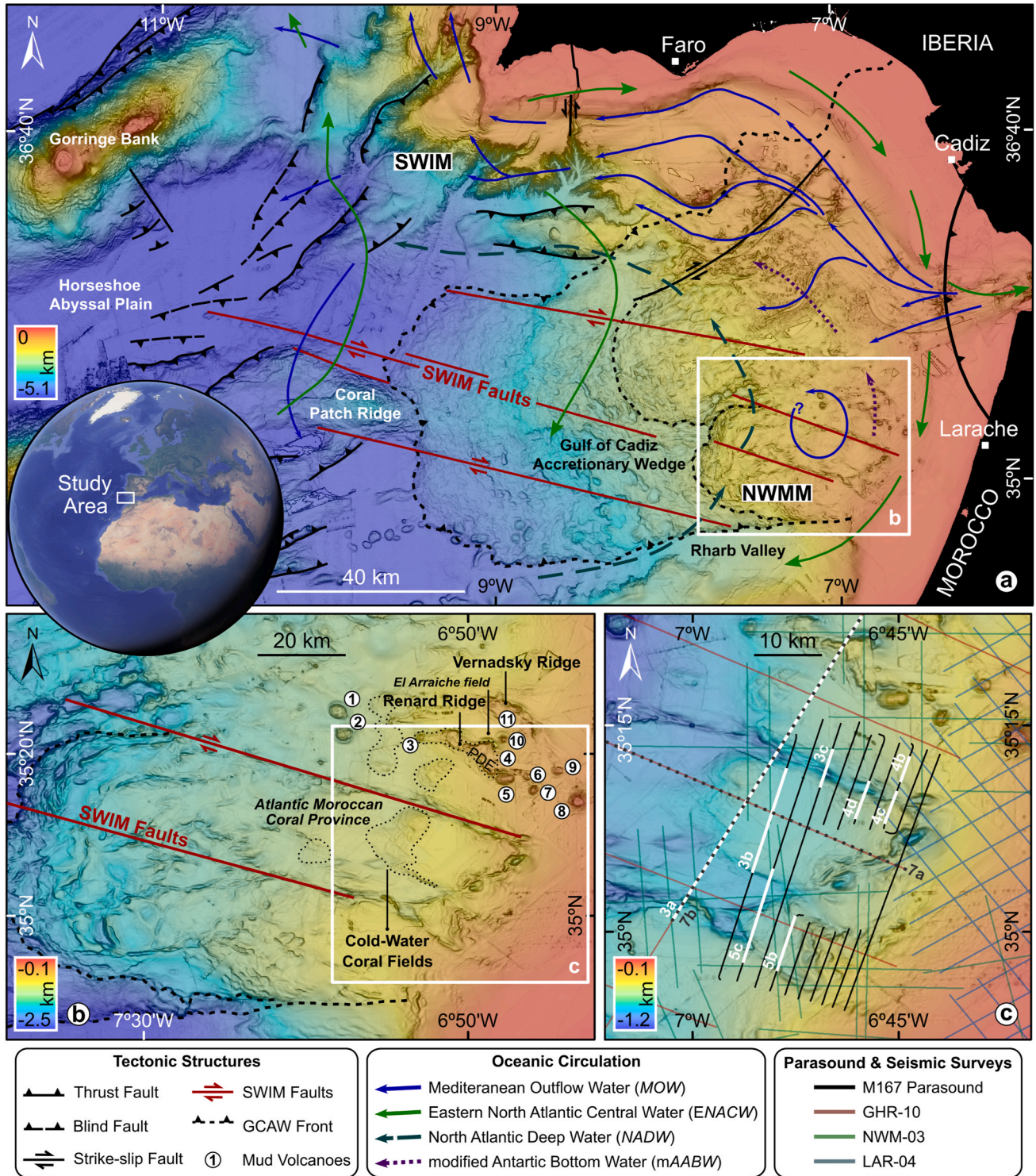
Fig. 1. *a)* Regional setting of the study area, showing the main structural features (Duarte et al., 2013; Cabral et al., 2017; Gamboa et al., 2021) and the distribution of the main intermediate- and deep-water masses along the Gulf of Cadiz (adapted from Hernández-Molina et al., 2011, 2016b; Vandorpe et al., 2014, 2016), SWIM: SW Iberian Margin, NWMM: NW Moroccan Margin; *b)* Detailed map of the NW Moroccan Margin (NWMM), showing the SWIM lineaments, cold-water coral fields (e. g., Hebbeln et al., 2016; Menapace et al., 2021) and fluid escape related features, the Vernadsky and Renard Ridges and several mud volcanoes (MV) recognised in the area: 1: Yuma MV, 2: Ginsburg MV, 3: TTR MV, 4: Lazarillo de Tormes MV, 5: Gemini MV, 6: Don Quijote MV, 7: Fiúza MV, 8: Il Idrissi MV, 9: Mercator MV, 10: Adamastor MV, 11: Kidd MV, PDE: Pen Duick Escarpment (Ivanov et al., 2000; Gardner, 2001; Van Rensbergen et al., 2003, 2005); *c)* Location of the parasound profiles (and 2D seismic datasets) used in the present study.

especially in the NW Moroccan Margin, also known as the Atlantic Moroccan Coral Province (Wienberg et al., 2009; Vandorpe et al., 2017, Fig. 1b). Oceanographic (e.g, water mass circulation and interface), sedimentary (e.g., contourite depositional systems), halokinetic (e.g., diapirs and associated fluid escape) and biogenic processes (cold-water coral mounds) are also important in this region (e.g., Medialdea et al., 2009; Mohn et al., 2014; Vandorpe et al., 2014, 2016; Hernández-Molina et al., 2016a, 2016b; Hebbeln et al., 2016, 2019; García et al., 2020).

An extensive contourite depositional system (CDS) developed along the northern slope of Gulf of Cadiz (i.e., the SW Iberian Margin), which has been widely studied over the past decades due to its considerable dimensions and (paleo)oceanographic implications (e.g., Nelson et al., 1999; Llave et al., 2001, 2007b; Roque et al., 2012; Hernández-Molina et al., 2003, 2016a; Duarte et al., 2022 and references therein). Contourites features have also been recognised in the southern Gulf of Cadiz (i.e., the NW Moroccan Margin), but have received far less attention in the literature. These have been linked with seafloor reliefs caused by mud volcanoes, scarps and ridges, such as in the El Arraiche area (Van Rooij et al., 2011; Vandorpe et al., 2014, 2016). Consequently, the Gulf of Cadiz, and specially its southern sector, is the ideal place to investigate the relation of along-slope circulation with the seafloor morpho-structural features.

The aims of this work are to study the spatial distribution of bottom-current (contourite) depositional and erosional features and thus, the interaction of (paleo)oceanographic processes with the morpho-tectonic seafloor relief in the NW Moroccan Margin (Fig. 1). To achieve this, high-resolution geophysical data were used consistent of multibeam bathymetry and parasound data acquired during the R/V METEOR "ALBOCA II" M167 cruise in 2020, complemented by high-resolution 2D seismic reflection data and the EMODnet bathymetric compilation (Fig. 1c).

2. Regional setting

2.1. Geological setting

The Gulf of Cadiz is located to the west of the Strait of Gibraltar between the southwestern continental margin of Iberia (SWIM, Fig. 1a) and the northwestern continental margin of Morocco (NWMM, Fig. 1a). This region is being influenced by the ongoing NW–SE to WNW–ESE Africa-Eurasia plate convergence at about 4.5–6.0 mm/yr (Stich et al., 2006; Zitellini et al., 2009; Cunha et al., 2012; Vergés and Fernàndez, 2012; Terrinha et al., 2019). The Africa-Iberia plate boundary is diffused, with deformation accommodated through strain partitioning along WNW–ESE dextral strike-slip faults (the SWIM lineaments; Fig. 1a and b) and NE–SW thrust faults (e.g., Rosas et al., 2009; Zitellini et al., 2009; Ramos et al., 2017b). The present-day kinematics commenced no later than 1.8 Ma with the latest Iberian-African plate boundary reorganization (Rosas et al., 2009). The SWIM faults, however, do not show significant seismicity, due to rheological weakening induced by fluid circulation and mantle hydration (Silva et al., 2017).

The Miocene collision between the African and Eurasian plates resulted in the development of the Betic-Rif orogenic system also known as Gibraltar Arc (e.g., Vergés and Fernàndez, 2012). The westward migration of the Alboran back-arc and Betic-Rif domain led to the formation of the Gulf of Cadiz Accretionary Wedge (GCAW) and the related gravitational allochthonous unit, during the Late Tortonian (Maldonado et al., 1999; Medialdea et al., 2004; Iribarren et al., 2007; Terrinha et al., 2019). It comprises a massive chaotic body of deformed Late Mesozoic-Cenozoic strata and its development was related to the eastwards dipping subduction of this oceanic lithospheric slab beneath the Gibraltar Arc (Gutscher et al., 2002; Terrinha et al., 2019). Due to the tectonic uplift of the Gibraltar Arc in the late Miocene, the marine connections of the Mediterranean Sea and the Atlantic Ocean (Betic and Rif Corridors and probably the Strait of Gibraltar, e.g., Krijgsman et al.,

2018) were progressively closed, triggering the Messinian Salinity Crisis (5.97–5.33 Ma; Flecker et al., 2015).

With the Pliocene reopening of the marine connection through the Strait of Gibraltar, the oceanographic setting of the region was controlled by the exchange between the Mediterranean Sea and Atlantic Ocean water masses (e.g., Rogerson et al., 2012).

Diapiric processes have been recognised throughout the Gulf of Cadiz, as a consequence of the vertical migration of Late Triassic-Hettangian evaporites and Miocene marls (Maestro et al., 2003; Medialdea et al., 2009; Matias et al., 2011; Flinch and Soto, 2017; Ramos et al., 2017a). Many fluid escape features have also been identified, such as mud volcanoes, pockmarks and extensive occurrences of methane-derived authigenic carbonates indicative of past and recent methane seepage at the seafloor (Ivanov et al., 2000; Gardner, 2001; Pinheiro et al., 2003; Van Rensbergen et al., 2003, 2005; Medialdea et al., 2009; León et al., 2010, 2012; Hensen et al., 2015; Magalhães et al., 2019; Xu et al., 2021). These features bear witness to the active fluid circulation throughout the southern Gulf of Cadiz, with shallow and deep origin (e.g., Hensen et al., 2015; Xu et al., 2021). Consequently, it is suggested the active role of the SWIM faults in facilitating deep fluid seepage. The interaction between tectonic, diapiric and fluid flow processes with bottom-current activity shape the seafloor morphology and thus influences the distribution of seafloor biologic communities (i.e., the cold-water coral mounds), deep-water sedimentation and gas hydrates (Wienberg et al., 2009, 2010, 2020; Vandorpe et al., 2014, 2016, 2017, 2023; Palomino et al., 2016; Magalhães et al., 2019; Lozano et al., 2020; Duarte et al., 2022).

2.2. Oceanographic setting

The present-day circulation pattern in the Gulf of Cadiz is mainly controlled by the exchange of Mediterranean Sea and Atlantic Ocean water masses through the Strait of Gibraltar (Ambar and Howe, 1979a, 1979b; Baringer and Price, 1999; Rogerson et al., 2012; Flecker et al., 2015). Several intermediate and deep-water masses play an important role in the oceanography of the region (Fig. 1a). In the Strait of Gibraltar, a two-layer circulation structure is recognised, with the flow of the warm, denser Mediterranean Outflow Water (MOW, 500–1400 m) into the Atlantic Ocean overlaid by the inflow of Atlantic waters into the Mediterranean Sea (Fig. 1a).

After exiting through the Strait of Gibraltar, the MOW spreads northwestwards along the SW Iberian middle slope (Fig. 1a), where it flows as an intermediate contour current between water depths of 500 and 1400 m (Sánchez-Leal et al., 2017) and led to the development of the extensive Gulf of Cadiz CDS (Llave et al., 2007a, 2007b, 2019; Roque et al., 2012; Hernández-Molina et al., 2016a, 2016b; Sánchez-Leal et al., 2017). Its interaction with the seafloor morphology causes the MOW to divide into two main branches (Ambar and Howe, 1979a, 1979b; Serra et al., 2005; Zenk and Armi, 1990): a less saline and warmer Upper Core (500–700 m) and a more saline and colder Lower Core (800–1400 m). The MOW is not deemed to be a constant water mass in the NW Moroccan Margin by several authors (e.g., Richardson et al., 2000; Ambar et al., 2008; Van Rooij et al., 2011), but it can be occasionally transported to the area through meddies at depths of ~1000 m. However, Lebreiro et al. (2018) suggest the influence of the MOW Upper Core, that mixes with Eastern North Atlantic Central Water (ENACW) and the modified Antarctic Intermediate Water (mAAIW), in the Moroccan middle slope. Furthermore, the ENACW and the mAAIW circulate over the MOW, at water depths of 100–600 m and 600 m and 1500 m respectively (Louarn and Morin, 2011; Hernández-Molina et al., 2014, 2016b; Roque et al., 2019).

Contourites features have also been recognised in the Moroccan Margin, in the El Arraiche area (Vernadsky and Renard Ridges in Fig. 1b), associated with mud volcanoes and ridges with seafloor relief and likely build up under the influence of the ENACW or the mAAIW (Vandorpe et al., 2014, 2016). Bottom-current circulation was also in

part responsible for the development of a large field of cold-water coral mounds, known as the Atlantic Moroccan Coral Province (Fig. 1b; Wienberg et al., 2009; Vandorpe et al., 2017).

3. Data and methods

3.1. Data

The dataset used in this work includes multibeam bathymetry, high-resolution Parasound echo-sounder profiles, 2D multi-channel seismic reflection profiles and hydrographic data (Fig. 1c).

Multibeam bathymetry acquired during the ALBOCA (M149, 25.072018–24.08.2018) and ALBOCA II (M167, 11.10.2020–05.11.2020) cruise (Hüpers et al., 2019; Menapace et al., 2021) covers the study area (Fig. 2a). It was acquired using a hull-mounted deep-water KONGSBERG EM122 system onboard the RV Meteor. The EM122 system used a nominal frequency of 12 kHz with a beam width configuration of 2° by 2°. The multibeam mapping was carried out with speeds of 8–10 knots. This bathymetric dataset was complemented with the EMODnet Digital bathymetric compilation, a publicly available seafloor bathymetry database, merging several high-resolution single and multiple beam bathymetric surveys with composite digital terrain models (EMODnet Bathymetry Consortium, 2018). It has a cell-size grid of ~115 m (pixel size of 1/16 arc minutes).

The 2D multichannel seismic reflection data include (in time domain; TWT – two-way travel time) profiles from three different surveys: GHR-10, NWM-03 and LAR-04 (Fig. 1c), acquired with an airgun array seismic source, processed to common depth point and stack, and time migrated using standard procedures (Hernández-Molina et al., 2016a and references therein; data courtesy of REPSOL, S.A.). Acquisition parameters for seismic surveys are detailed in Supplementary Material Table S1. Very high-resolution seismic data was acquired in the M167 cruise by a hull-mounted Atlas Parasound P70 sub-bottom profiler, operated to provide a high-resolution image of the uppermost 50–100 m of the sub-seafloor strata. It uses an operational signal (secondary low frequency) of 3.5 kHz, with a transducer array of 4° by 5° (Menapace et al., 2021).

Hydrographic data from World Ocean Database (2013) (https://www.nodc.noaa.gov/OC5/WOD13/) were used to create oceanographic sections of the NW Moroccan Margin. These were created based
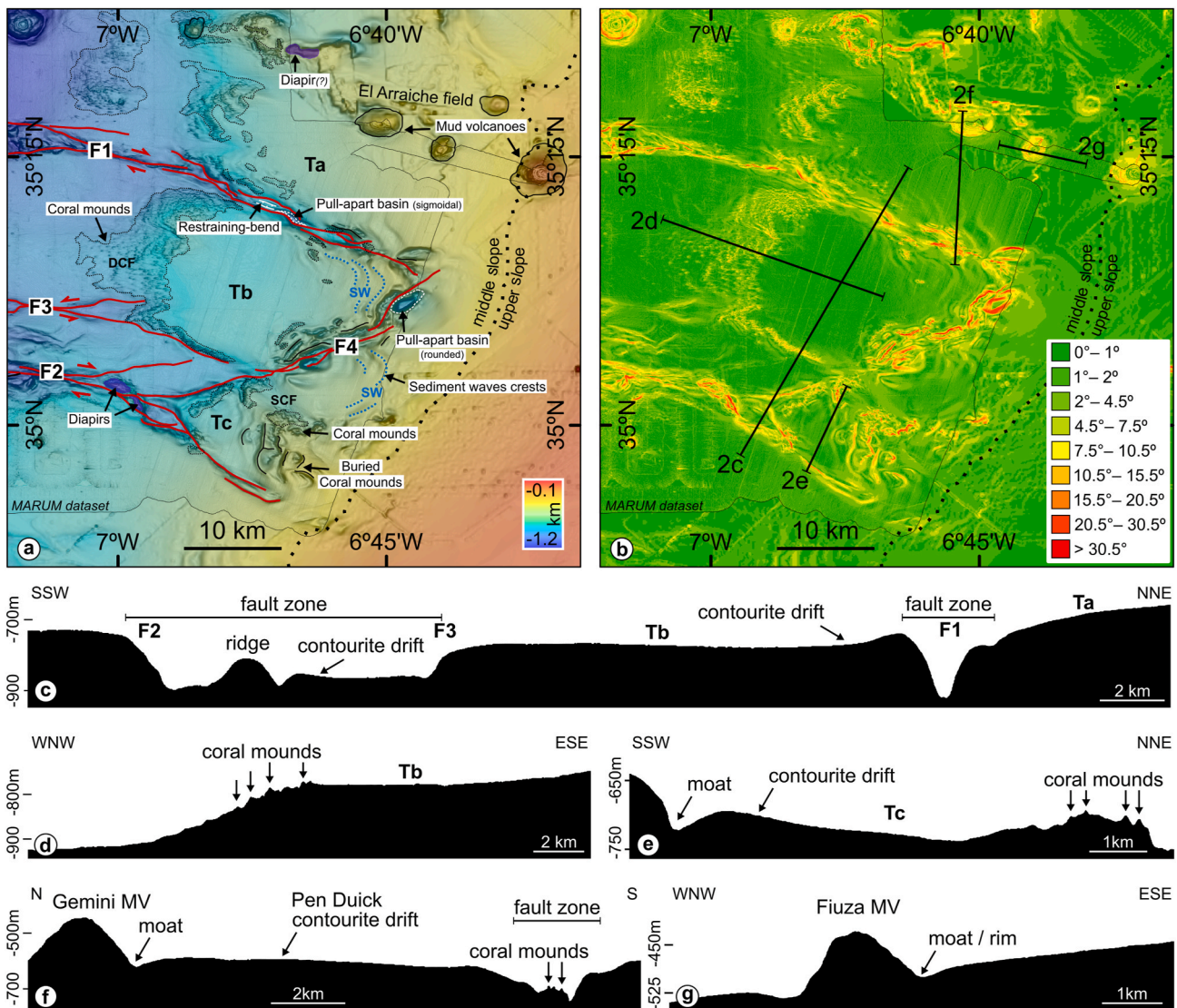

Fig. 2. Geomorphological characteristics of the NW Moroccan Margin: *a)* multibeam bathymetric map, with the main features identified in the different margin sectors (*F1, F2, F3, F4* faults, pull-apart basins (sigmoidal-to round-shaped depressions), Restraining-bends (topographic highs), contourite terraces *Ta, Tb* and *Tc,* mud volcanoes, corals mounds, and sediment waves; DCF: Deep Coral Field, SCF: Shallow Coral Field); *b)* slope gradients; *c)* to *g)* bathymetric profiles across the main morphological features of the study area. Pen Duick and Fiuza drifts are shown (Vandorpe et al., 2016). Location of the profiles is shown in Fig. 2b.

on analysis of CTD data (conductivity, temperature, and depth values) to display the detailed structure of the Present-day water masses in the study area.

3.2. Methods

The bathymetric dataset was used to perform a geomorphological analysis of the study area. Bathymetric maps and profiles, as well as slope gradients were made with the ArcGIS ArcMap software.

Seismic interpretation was performed using the Schlumberger Petrel E&P and IHS Kingdom Suite software. A time domain filter (2–6 kHz) and resampling (factor 2) were applied to the seismic data, and the profiles' envelope was calculated. A bandpass filter was applied to the profiles to improve the signal-to-noise ratio. Seismic interpretation followed the methodology proposed by Mitchum et al. (1977a, 1977b, 1977c) and Catuneanu et al. (2009). The age control of the multichannel 2D seismic was based on the correlation with seismostratigraphic analyses from previous studies in the region (Duarte et al., 2019; Ng et al., 2021a,b) – assigning an age of ~8 Ma to the seismic horizon TAP. The Parasound data interpretation followed the echo-type classification method established by Damuth and Hayes (1977), Damuth (1980), Kuhn and Weber (1993) and Droz et al. (2001), based on the geometry and internal configuration of sub-bottom reflections (i.e., acoustic amplitude, lateral continuity). The correlation of these echo-types with the bathymetric data was the base of the interpretation and discussion of the tectonic, sedimentary, and oceanographic processes acting in the study area. A simple conversion of TWT to depth was made, assuming a velocity of 1500 m/s for the first 50–100 of meters of the sedimentary cover. Hence, the sediment thickness is shown in meters.

Oceanographic analysis was performed using Ocean Data View (Schlitzer, 2015) to create temperature (θ), salinity (S) and potential density profiles. Considering the temperature (θ), salinity (S) and potential density values previously reported in the literature (e.g., Serra et al., 2005; Louarn and Morin, 2011; Hernández-Molina et al., 2014; Roque et al., 2019, 2023), 4 water masses were identified in the NW Moroccan Margin.

3.3. Terminology

Sediments deposited or substantially reworked by bottom-currents are known as contourites, and the large sedimentary accumulations they create are known as contourite drifts (sensu Faügères et al., 1999; Rebesco et al., 2014). These features are widely recognised along continental margins and in deep-water basins, in both passive and active tectonic settings (e.g., Van Rooij et al., 2003; Müller-Michaelis et al., 2013; Capella et al., 2017; Mulder et al., 2019; de Weger et al., 2020; Bailey et al., 2021). The identification of contourite features is based on the combination of seismic facies in associations with the three-dimensional depositional geometry (Miall, 1985; Nielsen et al., 2008; Rebesco et al., 2014). Contourite drifts can be classified based on variations in location, morphologies, size, sediment pattern, construction mechanisms and controls (Faügères and Stow, 2008; Rebesco et al., 2014; Duarte et al., 2022). Contourite erosional features, such as channels and moats, occur in association with the drifts in areas influenced by current cores, where the velocity is higher (García et al., 2009; Rebesco et al., 2014; Hernández-Molina et al., 2016a).

Coral mounds are composed of a mixture of coral fragments, other bioclasts and hemipelagic sediments (Dorschel et al., 2005). They develop in areas of vigorous bottom-current activity, as the currents transport food particles that maintain coral growth and sediment essential for mound growth (e.g., Vandorpe et al., 2017, 2023; Wienberg et al., 2010). In seismic data, the corals are characterized by transparent facies associated with diffraction hyperbolas and rooting on erosional surfaces (Hebbeln et al., 2016; Steinmann et al., 2020 and references therein). They are identified as elevated features above the seafloor (i.e., exposed mounds) or buried by continuous seismic reflections (i.e.,

buried mounds) (Steinmann et al., 2020 and references therein).

4. Results

4.1. Geomorphological features

The study area is located at water depths ranging between 108 and 1153 m (Figs. 1c and 2a). It comprises mainly the NW Moroccan continental middle slope, below depths of 400 m, but also the upper slope in the study area southeast corner (Fig. 2a). The area is characterised by a complex geomorphology, showing rough topography, with gradients higher than 10.5° (Fig. 2b). Smooth and gentle seafloor areas are also observed, with slope gradients ranging from 0° to 2° (Fig. 2b).

Several geomorphological features were identified during the analysis of the bathymetric (Fig. 2) and seismic data (multichannel and Parasound, Figs. 3–5), related to different processes such as structural (faults and diapirs), sedimentary (contourites and sediment waves), erosional (contourite channels and moats), mixed (contourite terraces), gravitational (slide scars, mass transport deposits), fluid migration (mud volcanoes and pockmarks) and biogenic (exposed and buried coral mounds). A detailed description of these features is given below.
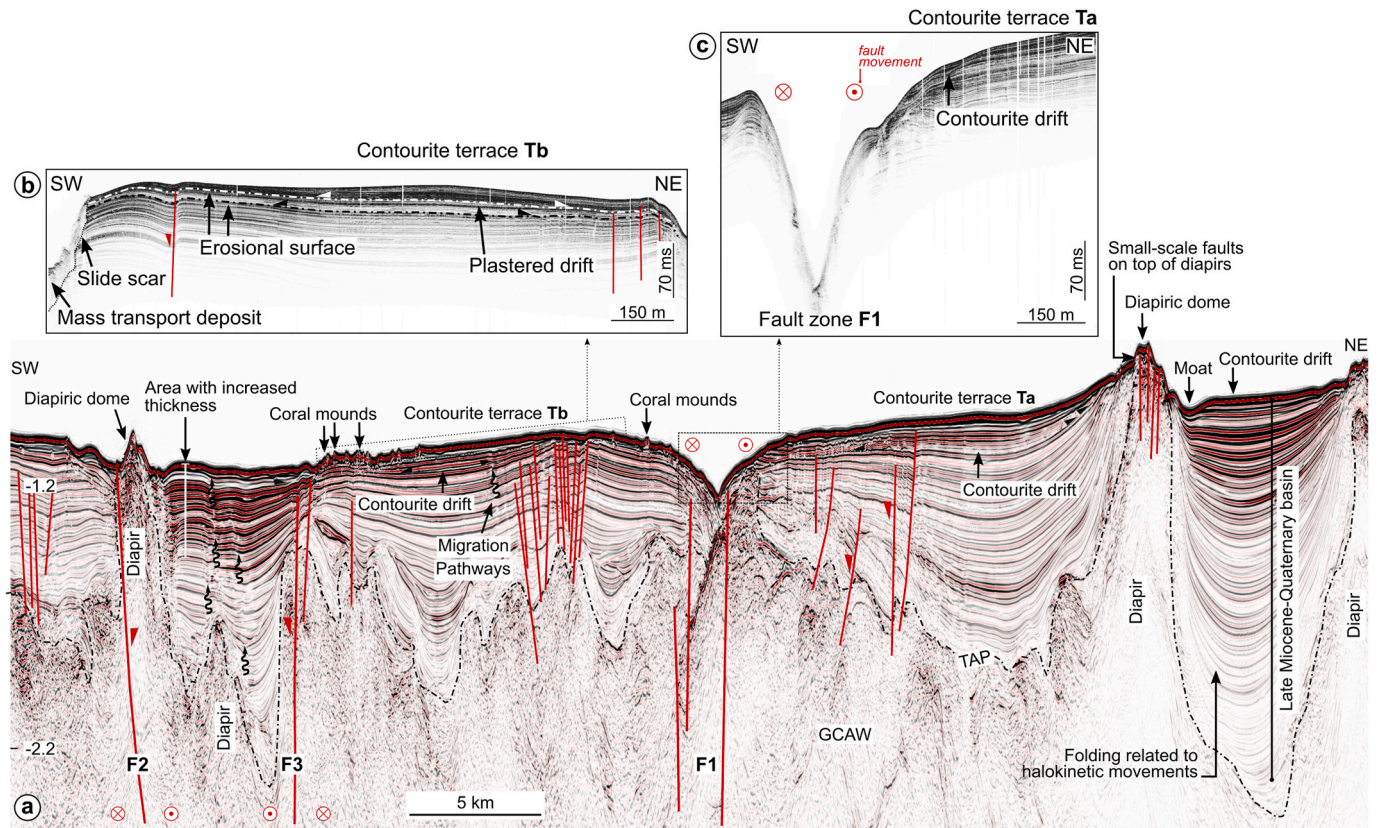
4.1.1. Structural features

4.1.1.1. Faults. The most prominent features observed in the bathymetry were four tectonic lineaments, two of them semi-parallel WNW-ESE-oriented (*F1* and *F2*, Fig. 2a) and two of minor dimensions (*F3* and *F4*, Fig. 2a).

F1 is observed over a length of 42 km (Fig. 2a) and it is characterised by symmetrical flanks (heights of 70 m) bounding a "v"-shaped depression (Figs. 2c, 3 and 4). Slope gradients in the *F1* fault zone can reach >10.5° (Fig. 2b). *F1* deforms the seismic sequence above the seismic horizon TAP, with a zone of discontinuous, faulted reflections (Fig. 3a). *F2* extends over ~43 km and shows an asymmetrical bathymetric imprint, with slope gradients varying from 4.5° to 7.5° in the south flank to >10.5° in the north flank (Figs. 2a and b, 6). Other minor faults were identified, namely *F3* located north of *F2* and extends throughout 24 km in a WNW-ESE direction (parallel to *F2*). This structure is less incised, resulting in slope gradients not exceeding 10.5° (Fig. 2a–c). The impact of *F2* and *F3* is shown by dip-slip displacement, bordering a depressed area where the seismic units show increased thickness (Figs. 3a, 5c). The last structure is *F4*, oriented ENE-WSW and showing a maximum length of ~23 km (Fig. 2a). It shows characteristics of a secondary shear fault, in relation to the main family of faults (*F1* and *F2*, Fig. 2a).

Throughout the fault zones, sigmoidal-to round-shaped depressions were recognised, corresponding to pull-apart basins (~2–5 km long, 2.5 km wide; Figs. 2a, c, 4c). Elongated topographic highs, can also be observed in the fault zones (~2–3.5 km long, 0.5–0.9 km wide; Fig. 2a and f). At depth, these structures are obscured by the chaotic nature of the GCAW, but it is still possible to observe several vertical to sub-vertical fault planes and a pop-up structure in Fig. 4d. These features are part of the previously described SWIM dextral strike-slip lineaments crossing the Gulf of Cadiz accretionary wedge (Fig. 1a and b; e.g., Rosas et al., 2009; Zitellini et al., 2009).

4.1.2. Halokinetic structures

Vertical halokinetic stocks with diffuse boundaries cutting through the late Miocene-Quaternary seismic section can be observed in the multichannel seismic (Fig. 3a). In some cases, they intrude through the sedimentary sequence, even showing seafloor expression observed as sub-rounded features in the bathymetric map (e.g., feature near *F2*, with 2 km length and 0.7 km wide; see diapirs in Figs. 2a and 3) and separating the margin into small depocenters (as observed in the synclinal basin in the north-western area of Fig. 3a). The diapirs are internally

Fig. 3. Correlation between a regional multichannel seismic profile (*a*) crossing the NW Moroccan Margin and parasound profiles (*b* and *c*, parallel to the multichannel profile), showing structural features (faults and diapirs), fluid flow features and cold-water corals. Several basins developed on top of the advancing orogenic wedge (GCAW). Sedimentary infill is composed of late Miocene to Quaternary deposits with a complex architecture (folding and tilting). Their evolution was controlled by halokinetic activity and fault movement, which led to the formation of sub-basins. The seismic profiles' vertical scale are in ms TWT. TAP: Top of Accretionary Prism (~8 Ma). Location of the seismic sections is shown in Fig. 1c. Red symbols indicate faults' movement.

characterised by transparent to chaotic internal reflections and very low to low amplitudes (Fig. 3a). These features are rooted in the GCAW and deform the overburden on top of the diapirs by folding or small-scale faulting (Fig. 3a).

Moreover, the 2D multichannel seismic profiles indicated that the halokinetic structures in the northern part of the study area compartmentalised the sedimentary sequence into different sub-basins characterised by stratified continuous, semi-parallel to parallel seismic reflections with amplitudes increasing from the base to the top (Fig. 3a). Internally, these basins show evidence of deformation, mainly by folding (syncline and anticline geometries) and small-scale normal faulting (Fig. 3a). Their top is marked by the Present-day seafloor, while the base is an irregular semi-continuous reflection (seismic horizon TAP), that separate them from chaotic to transparent reflections corresponding to the GCAW (Fig. 3).

4.1.3. Sedimentary features

Several depositional features, mostly related to bottom-water circulation (contourites and sediment waves), were recognised in the study area.

4.1.3.1. Contourites. Large, low-gradient areas (mostly <2°, locally <4.5°) slightly dipping seaward have been recognised along the NW Moroccan middle slope, forming a flatter domain with a terrace configuration at water depths between ~500 and 800 m (Figs. 2–5). The terrace (T) is divided and structured by the strike-slip faults *F1*, *F2*, *F3* and *F4* into three sectors – *Ta*, *Tb* and *Tc* in Fig. 2a. Terraces *Ta* and *Tb* are divided by the *F1* fault zone (Figs. 3, 4 and 7). Furthermore, *Tb* is bounded by *F3* at its southern border and *F4* to the east (Fig. 2a). Terrace

Tc is bounded by *F2* to the south and *F4* to the north (Fig. 2a). Terraces *Ta* and *Tb* show fairly similar characteristics, with a very flat seafloor with low slope gradients, while *Tc* shows a rougher topography. The morphologic characteristics of these features are shown in detail in Table 1.

In the seismic profiles, these areas are characterised by several packages of parallel to semi-parallel continuous low to high amplitude reflections (increasing to the top) with a general aggradational configuration (*Ta*, *Tb* and *Tc*) or locally with more mounded geometries (locally *Ta* and *Tc*) and onlapping and downlapping reflection terminations (Figs. 3–5). They were interpreted as plastered sheeted drifts, due to their geometry and internal characterisation (Table 1, Figs. 3b, 4c and 4d). These deposits are internally separated by seismic horizons with moderate to high amplitudes and are laterally continuous. Truncated reflections in the seismic record mark discontinuities interpreted as erosive surfaces (Figs. 3 and 4). This association of contourite depositional features (plastered drift) and erosional episodes allows the identification of *Ta*, *Tb* and *Tc* as contourite terraces, first order morphological features of a contourite system.

Furthermore, mounded bodies are observed developing at the base of structural highs, at water depths below 850 m and rising 10–40 m above the surrounding seafloor (Table 1, Figs. 2c, e, f, g, 5). They are separated from the structural highs by depressions with 'u'-shaped profiles in cross-sections, interpreted as moats (Figs. 2c, e–g, 5a–c). In some cases, these mounded deposits are bordered by erosional features on both sides (Figs. 3 and 5c). Based on their geometry and internal configuration (Table 1, Fig. 5b and c), these deposits have internal geometries and typical features of contourite mounded and confined mounded drifts and are considered as secondary smaller features.
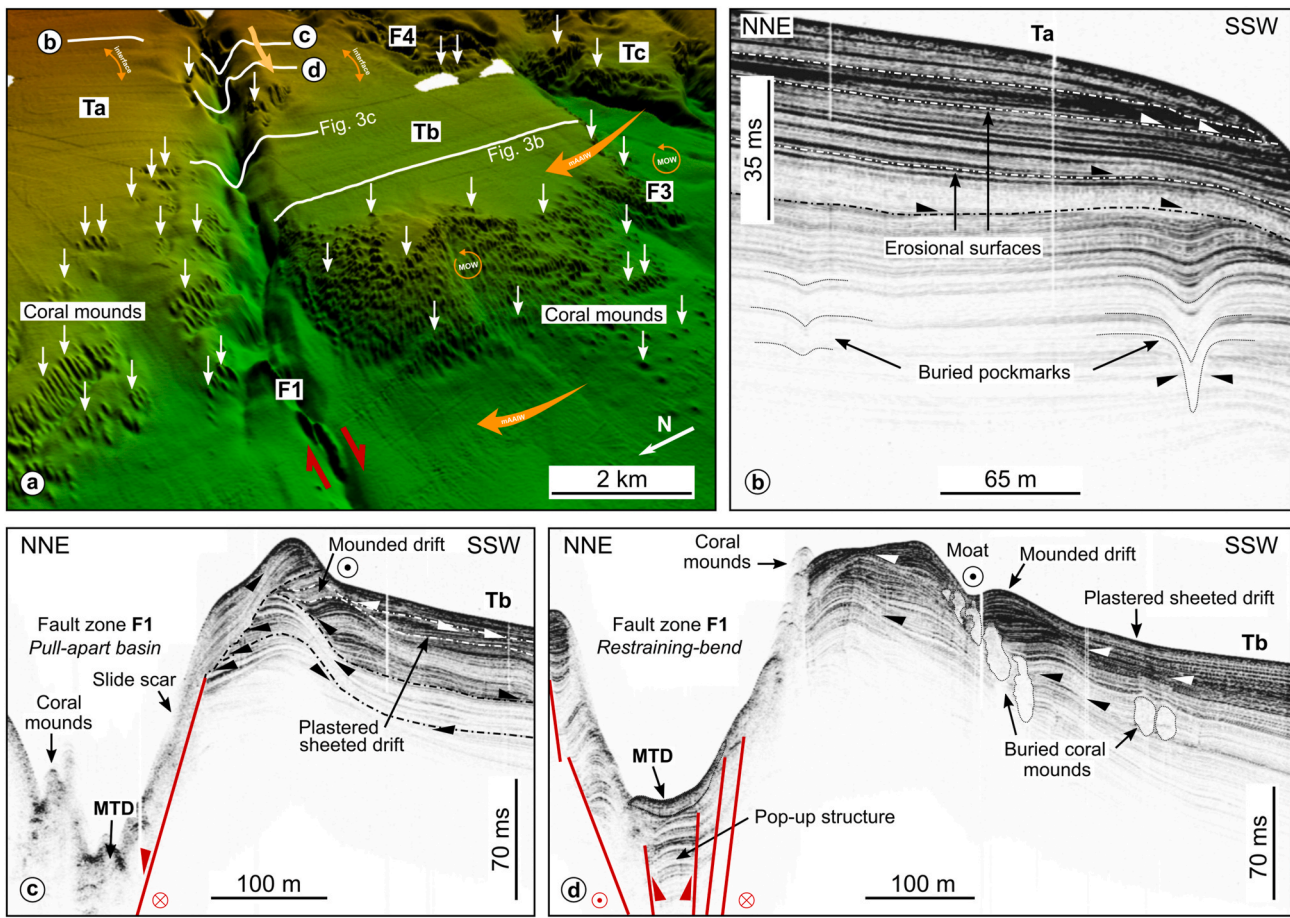
Fig. 4. Geomorphological characterisation of the northern part of the study area: *a)* bathymetric map showing the tectonic structures (*F1, F3* and *F4*) and cold-water coral mounds (white arrows) associated with the contourite terraces *Ta* and *Tb*. *b)* to d) parasound echo-sounder profiles displaying the morphology and sub-seafloor geometry, with contourite depositional and erosional features, buried and exposed cold-water corals and buried pockmarks. Location of seismic profiles in Fig. 1c. A version without interpretation is shown in the supplementary materials (Fig. S1).

4.1.3.2. Sediment waves. These features were punctually recognised along the contourite terrace, at water depths of ~500–650 m (Figs. 2a and 6). They are elongated along a general NNE-SSW direction and create undulated fields at the seafloor (Fig. 2a). In the seismic data they are characterised by parallel to sub-parallel continuous reflections with low to moderate amplitudes and form symmetrical to slightly sigmoid-shaped layers (Fig. 6). They show maximum wavelengths of 0.78 km and heights up to 30 m (Fig. 2a and b, Table 1). These features were interpreted as sediment waves.

Two fields of sediment waves were recognised: the first one occurs at the eastern part of the contourite terrace *T2*, between *F1* and *F4* at water depths of 600 m–725 m (Fig. 2a), and a second one in the upper part of the middle slope to the east of *F4* and northeast of contourite terrace *T3* (Fig. 2a) at water depths of 525 m–650 m.

4.1.4. Erosional features

Elongated depressions with 'v' and 'u' shaped profiles often occur along the base of the seafloor highs in the NW Moroccan Margin (Table 1), such as the SWIM faults (Figs. 3 and 5) or folded areas (Figs. 3 and 4).

The 'v'-shaped features are narrow depressions, with vertical incisions reaching 36 m and widths of 0.2–0.4 km (Figs. 2, 5b and 5c). They show a general NW-SE orientation and were identified as contourite channels in this study. The 'u'-shaped features show widths of 0.1–1.2 km and vertical incisions up to 17.5 m (Figs. 4 and 5). They develop in an approximate NW-SE direction and are associated with mounded and confined drifts that form on the right side of these features

(Fig. 5). These erosional structures were identified as contourite moats due to their characteristics and relationship with contourite drift deposits (Figs. 2, 3 and 5).

4.1.5. Gravitational features

4.1.5.1. Mass transport deposits. Lens to wedge-shaped transparent to chaotic facies bodies were recognised in the seismic data, at the foot of the fault scarps (Table 1, Figs. 4 and 5). These deposits occur mainly at the Present-day seafloor, with predominantly chaotic facies (thickness between 7.5 m and 9.8 m and lengths of 75 m–80 m) but can also be identified in the subsurface as transparent wedge-shaped deposits (thickness between 6.8 m and 11.3 m and lengths of ~30 m–40 m) intercalated with the stratified contourite deposits (Fig. 5).

4.1.5.2. Slide scars. Steep slope areas (7.5° to >10.5°, Fig. 2b) are located in the headscarp of the mass transport deposits described above (Table 1, Figs. 2b, 3 and 4). In these areas the seafloor is marked by a moderate to high amplitude discontinuous reflection that truncates the older layered seismic reflections (Figs. 3 and 4), or the sub-bottom reflections are just absent (Fig. 5).

4.1.6. Fluid migration features

In the north-eastern region of the study area nine circular to elongated positive reliefs can be observed at water depths below 500 m (Fig. 2a). These features rise 25–232 m from the surrounding seabed, have diameters ranging from 1 to 4.9 km and border slopes ranging from
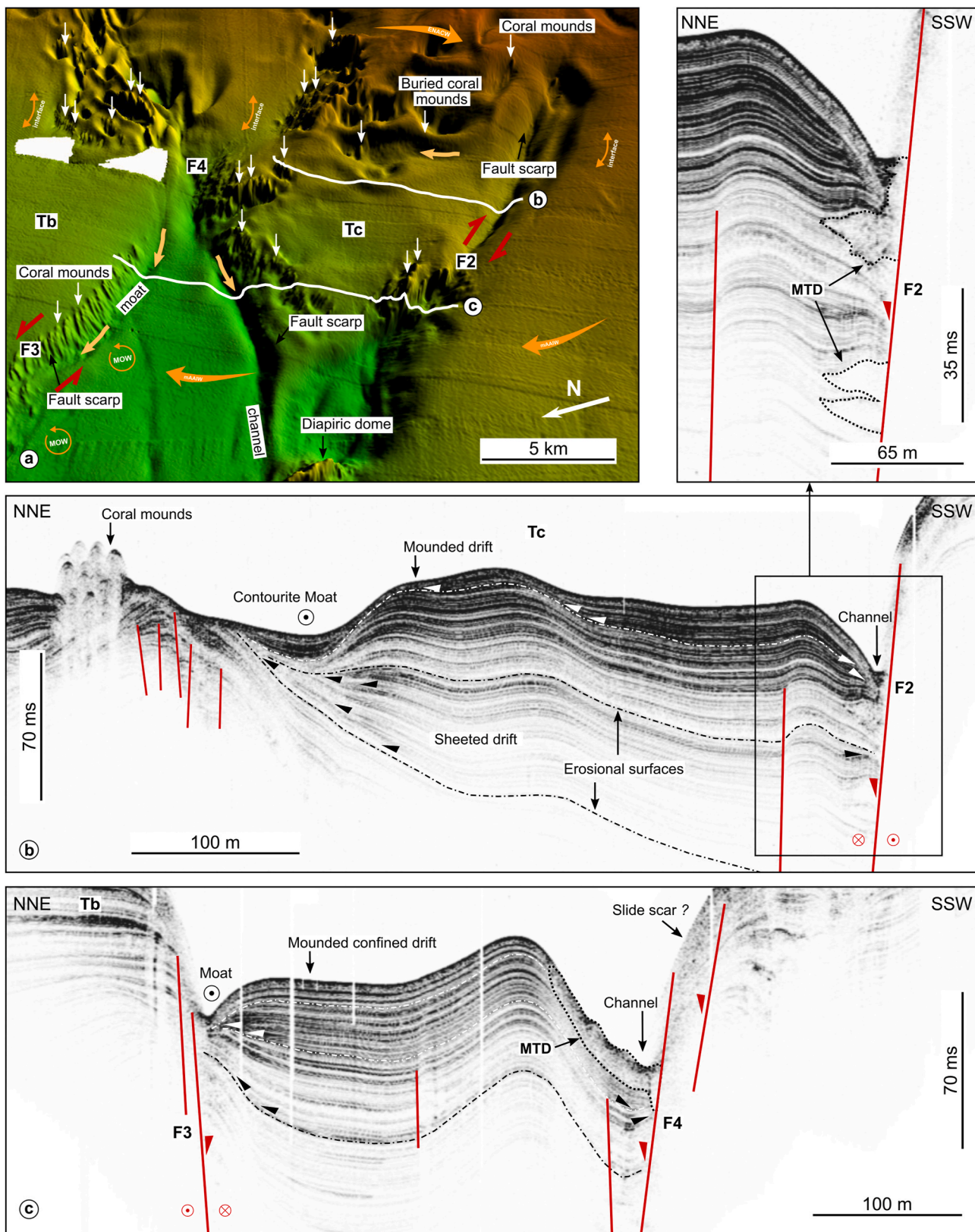
Fig. 5. Geomorphological characterisation of the southern part of the study area: *a)* bathymetric map showing the tectonic structures (*F2, F3* and *F4*) and cold-water coral mounds (white arrows) associated with the contourite terraces *Tb* and *Tc*. Blue arrow: water masses pathways; *b)* and c) parasound echo-sounder profiles displaying the morphology and sub-seafloor geometry, with contourite depositional and erosional features, cold-water corals and gravitational features (mass transport deposits and slide scars). Location of seismic profiles in Fig. 1c. A version without interpretation is shown in the supplementary materials (Fig. S2).
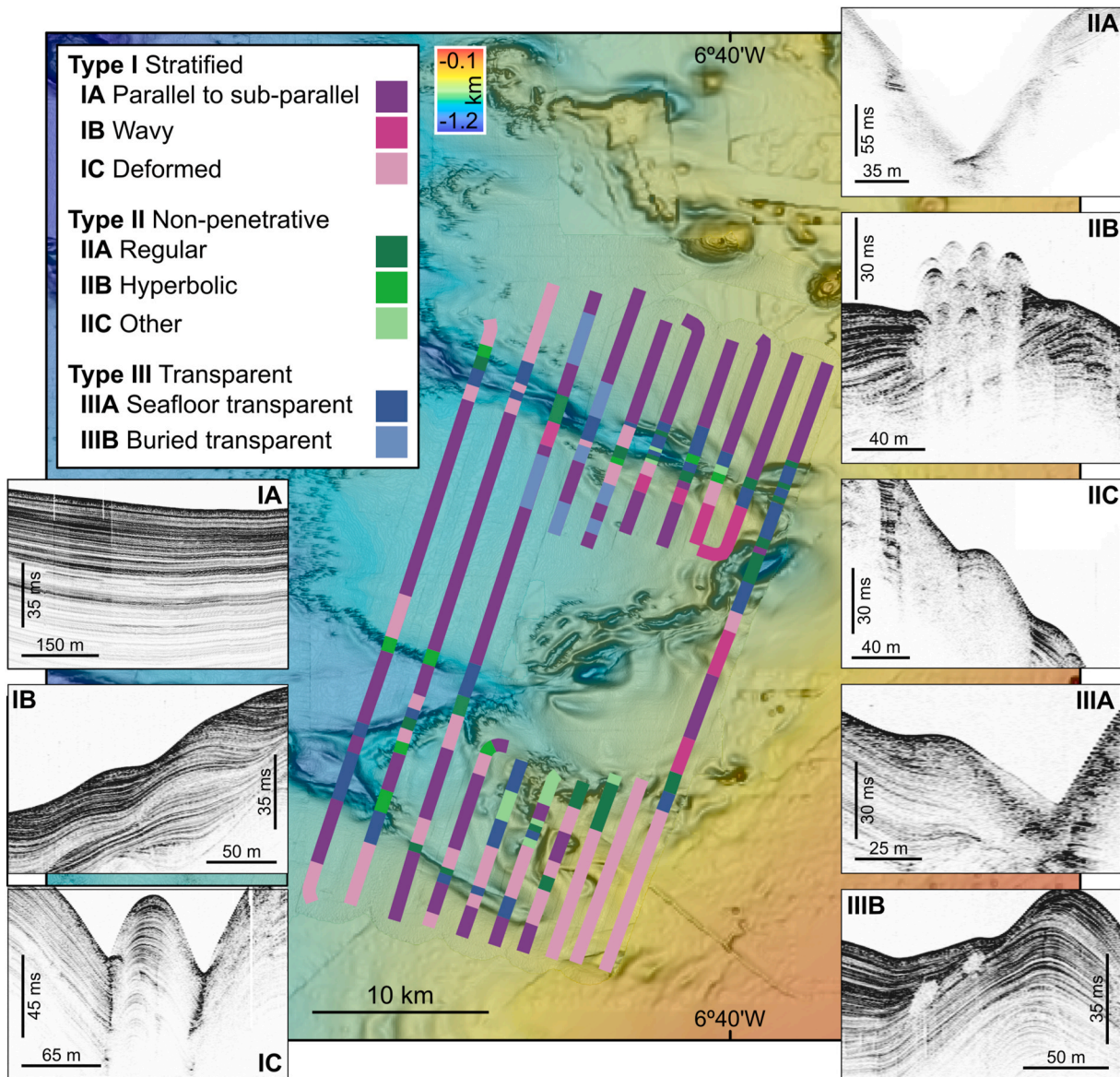
Fig. 6. Distribution map of the echo-types identified in the NW Moroccan Margin, with parasound sections showing examples of the echo-types.
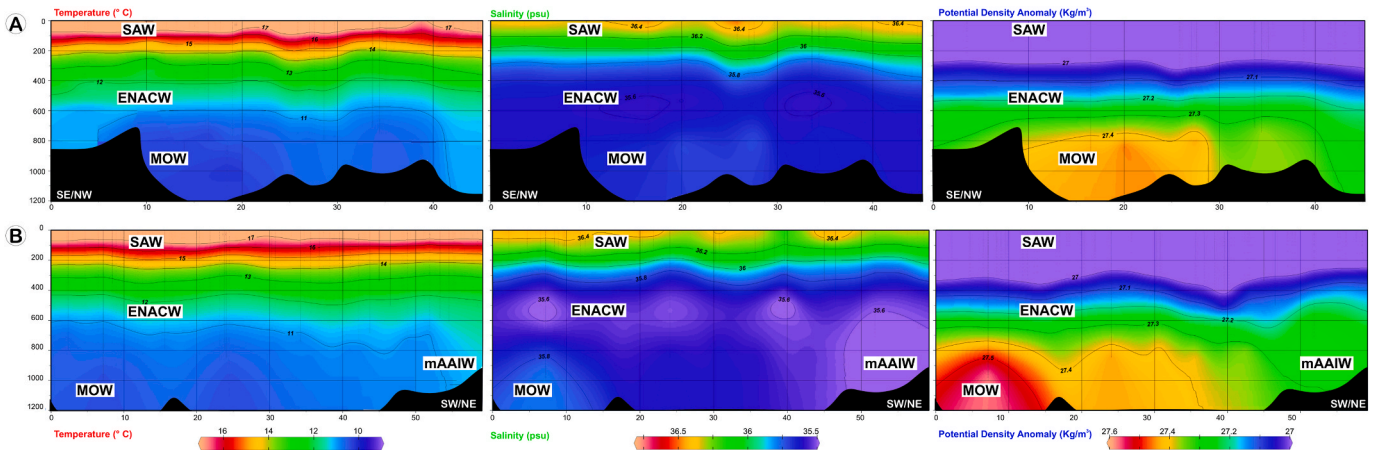

Fig. 7. Hydrographic sections of the study area showing the temperature (°C), salinity and potential density values (σ, Kg/m3) as well as the interpretation for the main regional water masses and their boundaries.

Table 1
Morphologic characteristics of the geomorphological features recognised in the study area. E: Exposed, B: Buried, ms: milliseconds in TWT. NEW TABLE!

PROCESS	GEOMORPHOLOGICAL FEATURES		GEOMORPHOLOGICAL PARAMETERS					
			Form	Length	Width	Height/ Thickness	Trend	Slope gradient
Structural	Faults	F1	-	42 km	-	-	WNW- ESE	>10.5°
		F2	-	~43 km	-	-	WNW- ESE	N flank >10.5° S flank 4.5°-7.5°
		F3	-	24 km	-	-	WNW- ESE	<10.5°
		F4	-	~23 km	-	-	ENE- WSW	>10.5°
	Diapirs	E	Sub-circular to elongated	2 km	0.7 km	~75 m	WNW − ESE?	up to >30.5°
		B		~75 m	~75 m	>1.1 m	WNW − ESE?	-
Sedimentary	Contourites		Plastered sheeted	3.4-24 km	2.7-15 km	16-34 m	-	0°-2°
			Mounded	2.3-13.7 km	1.3-6 km	32-87 m	-	0°-2°
			Confined	4-8 km	4-10 km	21-53 m	-	0°-2°
	Sediment waves		Undulated	~14-17 km	~30-60 km	up to 30m	NNE- SSW	0°-4.5°
Erosional	Contourite channels		'v'-shaped	-				NW- SE	2°-4.5°
	Contourite moats		'u'-shaped	-				NW- SE	2°-4.5° (<7.5°)
Mixed	Contourite terraces	Ta	Rectangular					-	0°-2°
		Tb	Trapezoidal					-	0°-2°
		Tc	Triangular					-	<4.5°
Gravitational	Slide scars		-	-	-	-	-	7.50°-10.5°
	Mass transport deposits	E	Lens to wedge-shaped	75 to 80 m	-	5.6-7.3 m	-	-
		B	Wedge-shaped	~30 to 40 m	-	5-8.4 m	-	-
Fluid migration	Mud volcanoes		Circular to elongated	1-4.9 km		25-232 m	-	6.8°-8.4°
	Pockmarks		'u' & 'v'-shaped	61-260 m		7.5 m	-	-
Biogenic	Exposed corals		Circular to oval	~540-880 m		up to 19 m	-	-
	Buried corals			5-12 km		6-30 m	-	-
				Diameter				

6.8° up to 8.4° (Table 1, Fig. 2b). In cross-sections, they are characterised by cone-shaped profiles (Fig. 2f and g). In some cases, it is possible to observe a depressed area (11 m–39 m depth) around the structures rim (Fig. 2a, f, g). These features occur near the northern boundary of the study area, in the El Arraiche field (Fig. 2a) and are associated with the previously recognised mud volcanoes in this region (e.g., Gardner, 2001; Pinheiro et al., 2003; Van Rensbergen et al., 2005; Vandorpe et al., 2016).

More evidence for fluid flow processes can be observed in the seismic profiles: *i)* three buried crater-like depression with 'u'- and 'v'-shaped profiles were observed in the northern part of the study area (Table 1, Fig. 4). These depressions have depths up to 0.01 s TWT, with diameters ranging from 61 to 260 m. These features display geometries compatible with pockmarks produced by fluid seepage at the paleo-seafloor; and *ii)* areas of acoustic disturbed reflections can be recognised throughout the profiles (Fig. 3), such as vertical zones of acoustic wipe-out, characterised by low amplitude to transparent reflections.

4.1.6.1. Coral mounds. Multiple positive conical-shaped features are observed in the bathymetry between water depths of ~540 up to 980 m (Fig. 2a and b). In the parasound seismic profiles they exhibit circular to oval or vertically elongated shapes with transparent facies (Table 1, Figs. 4 and 5), or small triangular bumps on the seafloor in the regional multichannel seismic (Fig. 3). These structures are characterised by diameters ranging from ~130 to ~235 m and highs up to 19 m above the surrounding seafloor. They are observed along zones of breaks in the slope gradient (Fig. 2a, b, d), in areas where the seabed is steeper (slopes of 7.5°–10.5°, Fig. 2b). They can occur isolated or in groups, parallel to the slope (Fig. 2a and d), at bathymetric highs (Fig. 2a and e) or within the fault lineaments (Fig. 2a and f). Based on their acoustic characteristics these features are interpreted as cold-water coral mounds. These features were previously recognised and described in depth by Hebbeln et al. (2016, 2019).
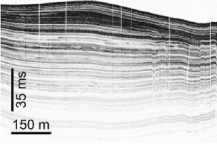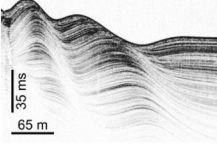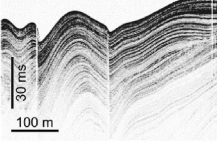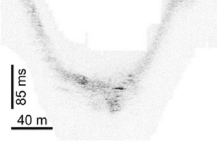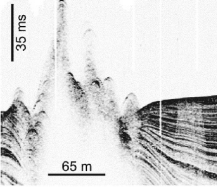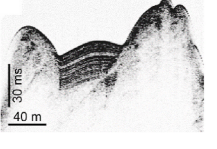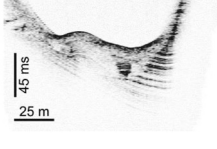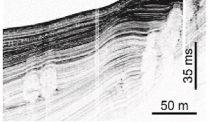
Two different coral mound fields with different characteristics were recognised: *i)* the deeper field occurs along an extensive area between water depths of 800–980 m (DCF in Figs. 2a and 8). It consists of a group of exposed cold-water coral mounds developed in an area where the seabed changes from a smooth flatten terrace to a steeper slope configuration (Fig. 2a, b, d), and *ii)* the shallower field is observed at water depths of ~540–760 m (SCF in Figs. 2a and 8). It is characterised by some exposed conical-shaped mounds developing especially in the fault zones, but also by several 5–12 km length ridges with similar orientations to the coral mound groups (Fig. 2a). These ridges are thus suspected to be related with buried coral mounds. Buried corals (Fig. 4d) are also observed in the parasound profiles, at different levels of the sedimentary sequence, suggesting several formation episodes (Vandorpe et al., 2017).

4.2. Echo-type characterization

Three main echo-types – stratified, non-penetrative and transparent – are distinguished based on the acoustic characterisation of the parasound seismic profiles. The echo-types are described in detail on Table 2, and their distribution is shown in Fig. 6.

Table 2
Echo-types identified in the NW Moroccan Margin: description and possible interpretations for the echo-types observed in the parasound profiles.

Echo-types		Example	Description	Interpretation
Type I – Stratified	*IA*		Continuous sharp seafloor reflection. Package of parallel, well-stratified continuous reflections with amplitudes decreasing with depth, from high to low.	Hemipelagic or contourite deposits
	IB		Continuous sharp seafloor reflection. Undulated well-stratified and sub-parallel, continuous reflections. High to low amplitudes, decreasing with depth.	Sediment waves
	IC		Sharp seafloor reflection. Well-stratified and sub-parallel, semi-continuous reflections, with folds and faults that deform the whole package. High to low amplitudes.	Folded and faulted sedimentary deposits
Type II – Non-penetrative	*IIA*		High amplitude sharp reflection. Occurs on steep slope areas. Sub-bottom reflections are absent.	Erosional processes (slope failure or by bottom-currents)
	IIB		Conical-shaped features, with the seafloor marked by weak diffraction hyperbolas. Transparent internal facies. Laterally, it borders continuous stratified reflections (echo-type I).	Cold-water coral mounds
	IIC		Sharp seafloor echo with irregular and overlapping hyperbolas without sub-bottom reflections.	Partially buried cold-water coral mounds
Type III – Transparent	*IIIA*		Sharp continuous seafloor reflection. Lens external geometry, with transparent to chaotic facies.	Mass transport deposits
	IIIB		Transparent to chaotic facies with mounded geometries. These are surrounded by continuous stratified reflections (echo-type I).	Buried coral mounds

4.3. Oceanographic profiles

Two hydrographic sections were created based on analysis of CTD data to display the structure of the water masses along the study area, one section perpendicular to the slope (NW – SE, Fig. 7a) and the other parallel (NE – SW, Fig. 7b). Based on the temperature, salinity and potential density values observed, four water masses were identified: *i)* the Surface Atlantic Water (SAW) is the most superficial water mass in the study, reaching around 200 m water depths, *ii)* the Eastern North Atlantic Central Water (ENACW), directly below the SAW, and going down to ~500–600 m. It is characterized by a temperature of 13.9 °C, a salinity minimum of 36.289 and an oxygen content of 180 μmol/kg. The ENACW is affected by eddies, as can be identified on Fig. 7b, *iii)* the modified Antarctic Intermediate Water (mAAIW), is observed between ~500 and 600 and 1000 m water depths (Fig. 7). It is characterized by a temperature of 16.374 °C, a salinity minimum of 35.62 and an oxygen content of 225.93 μmol/kg (see Figs. 4 and 5 of Roque et al., 2019), with its main core located at 900 m (Fig. 7). It spreads along the African continental margin until the Gulf of Cadiz (Louarn and Morin, 2011; Hernández-Molina et al., 2014), where it interacts with the

Mediterranean Outflow Water (Roque et al., 2019, 2023), and *iv)* the Mediterranean Outflow Water (MOW), that flows directly below the ENACW (below 800 m), and is characterised by a temperature of 13.9 °C, a salinity minimum of 36.64 and an oxygen content of 180 µmol/kg (Roque et al., 2019). The MOW core position is restricted by seafloor irregularities (Fig. 7), with local maximum and doming upper surface. It transitions laterally to the mAAIW and is also affected by the eddies observed in Fig. 7b.

5. Discussion

The distribution of geomorphological features in the study area discloses the interplay of tectonic and oceanographic processes in the NW Moroccan Margin. The sedimentation is dominated by bottom-current related deposits, with an extensive contourite terrace along the middle continental slope and associated sheeted drifts and sediment waves. Mounded to confined drifts and erosive contourite features were also locally recognised, as well as mass transport deposits. The distribution and the type of the deposits are closely influenced by the morpho-structural reliefs (Figs. 3–5, 8).

Although no direct chronostratigraphic control is available due to the lack of wells in the study area, a theoretical late Quaternary age is proposed for the studied seismic interval based on regional data existent in the literature. Accordingly, a 0.9–0.7 Ma to Present age is attributed
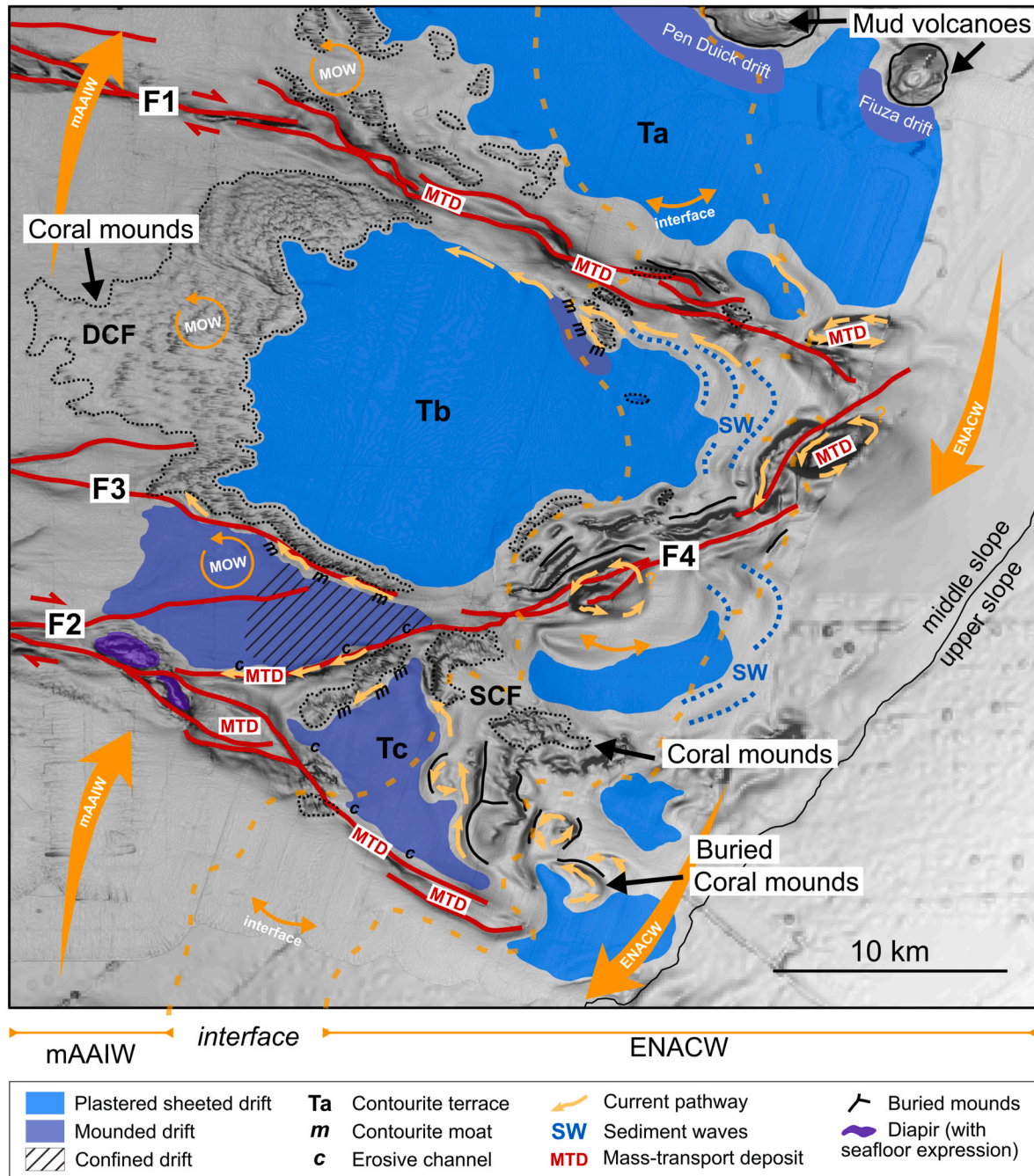

Fig. 8. Map showing the distribution of the geomorphologic features (faults, diapirs, contourites, sediment waves, cold-water corals and gravitational) observed in the NW Moroccan Margin. The distribution of the contourite depositional and erosional features were used to infer bottom-current pathways during the Late Quaternary (light orange arrows). F1, F2, F3, F4: strike-slip faults, Ta, Tb, Tc: Contourite terraces, MTD: Mass-transport deposit, SW: Sediment waves, DCF: Deep Coral Field, SCF: Shallow Coral Field, *m*: contourite moat, *c*: erosive channel. Pen Duick and Fiuza drifts from Vandorpe et al. (2016).

for the interval of interest based on chrono-seismostratigraphy proposed for the Moroccan margin (Vandorpe et al., 2014). Furthermore, the high-resolution seismic (Parasound) record images the first tens of meters below the seafloor, usually corresponding to sediments no older than Late Quaternary (e.g., Droz et al., 2001), as has been proposed in the northern Gulf of Cadiz (e.g., Llave et al., 2001, 2006; García et al., 2020).

5.1. Morpho-structural control on sedimentation and coral distribution

The seafloor morphology of the study area is mainly influenced by a set of strike-slip faults, namely the SWIM and associated faults (*F1*, *F2*, *F3* and *F4* in Figs. 2a and 8). Mud volcanoes are also locally important in shaping the seafloor (sector 1, Fig. 2) and thus controlling depositional processes. Tectonic control on sedimentary processes is observed, with several sedimentary sub-basins developed on top of the GCAW and compartmentalised by diapiric structures or the fault zones (Fig. 3a). All these structures impact the late Quaternary seismic sequence (folds and small-scale faults, Fig. 3), characterised by echo-type *IC* (Table 2, Fig. 6), indicating the importance of tectonic activity, halokinetics and consequent deformation on the recent evolution of the NW Moroccan Margin.

Internal deformation of the seismic strata is more intense in the southern part of the study area (sector 3, Fig. 2a), where echo-type *IC* dominates (Table 2, Figs. 5 and 6). This suggests a higher activity of faults *F2*, *F3* and *F4* or just a different setting: movements in *F1* appear to be closer to pure strike-slip, with the typical pull-apart basins and restraining-bends structures developing within the fault zone (Figs. 2a, 4c and 4d), while in the southern part of the study area the faults seem to accommodate deformation as a group and important dip-slip movement is observed in *F2*, *F3* and locally in *F4* (Figs. 3 and 5).

The observed deformation is a consequence of the regional tectonics, with structures within the GCAW still showing evidence of local activity (Gutscher et al., 2009; Duarte et al., 2022) and the SWIM faults marking the diffuse boundary between the African and European plates, characterised by a dextral transpressive regime in the last 1.8 Ma (Rosas et al., 2009; Zitellini et al., 2009; Terrinha et al., 2019). Recent tectonic activity is also demonstrated by the formation of salt structures rooted in the GCAW (Figs. 2a, 3a and 8) and the fluid escape features, both in the recent record – the buried pockmarks seen in Fig. 4b – and at the Present-day – the mud volcanoes to the north of the study area (Fig. 2, Perez-Garcia et al., 2011; Vandorpe et al., 2014, 2016; Xu et al., 2021).

The changes caused on seafloor morphology, in particular by the SWIM faults' scarps (i.e., zones of high slope gradient, Fig. 2b), influence sedimentation in several ways: *i)* restricting sedimentary deposits extension, controlling the available accommodation space (Figs. 3–5, 8) and *ii)* creating slope instabilities that cause the development of mass transport deposits (Figs. 3–5). Slope instability was only recognised on the steep slope areas related to the fault scarps (i.e., zone of high slope gradient, Figs. 3 and 4). In these areas, echo-type *IIA* is observed (Table 2, Fig. 6), characteristic of areas with sediment failure (e.g., Roque et al., 2022). At the base of the steeper scarps (pull-apart basins), echo-types *IIIA* (Table 2, Fig. 6) were observed with chaotic lense-shaped bodies and no internals structures that are related to mass transport deposits.

The morpho-structural control on seafloor configuration is also important for the coral mounds distribution along the NW Moroccan margin, with some of these features occurring along fault scarps (Figs. 2a, 4, 5 and 8). These areas are characterised by high slope gradients and thus, the mounds are better exposed to passing water masses that are enhanced by the seafloor morphology and are rich in nutrients (Hebbeln et al., 2019 and references therein).

5.2. Bottom-current depositional and erosional processes

Contourite features are dominant in the study area. In the seismic profiles, contourite deposits correspond mainly to the stratified echo-type *IA*, but also echo-type *IC* if the sedimentary sequence suffered significant deformation (Table 2, Fig. 6). Three contourite terraces were recognised (*Ta*, *Tb* and *Tc* in Figs. 2a, 3 and 8), separated by the strike-slip faults and thus showing the importance of the SWIM faults, local halokinetic and fluid flow processes shaping the morphology of the study area (details in *6.1*). These terraces are characterised by an association of depositional elements – such as contourite drifts (Table 1, Figs. 3–5) and the recognised sediment waves, corresponding to the wavy stratified echo-type *IB* (Table 2, Fig. 6) and paleo-erosional features, such as discontinuities in the seismic record (Fig. 3). This demonstrates the variability of bottom-current associated processes during the late Quaternary in the study area. Contourite terraces have been documented across the world, such as in Mozambique Channel (Miramontes et al., 2021), Uruguayan Margin (Hernández-Molina et al., 2018; Kirby et al., 2021) and South China Sea (Chen et al., 2022), being interpreted as shaped in the transitional domain between two different water masses (Preu et al., 2013). To the south of contourite terrace *Tb*, mounded and confined mounded drifts are observed (Figs. 5b and c, 8). These deposits are separated from the contourite terrace by a fault scarp, developing at the base of *Tb* at deeper depths. Landward, another field of sediment waves were recognised together with sheeted drifts, revealing bottom-current activity in the upper part of the middle slope (Figs. 2a and 8). The formation of the sediment waves suggests turbulent mixing between the water masses, with internal waves fluctuating along the pycnocline (Rebesco et al., 2014; Yin et al., 2019; Roque et al., 2023). In this situation, the high velocity and energy of the internal waves are likely to create local erosion of the seafloor and sediment re-suspension (Pomar et al., 2012; Ribó et al., 2018; Mienis et al., 2009). These contourite features, together with the drifts recognised previously in the El Arraiche area to the north (Pen Duick and Fiuza drifts in Vandorpe et al., 2014, 2016), form an important contourite system along the NW Moroccan Margin middle slope (Fig. 8).

As stated above, the morpho-structural characteristics of the seafloor condition the formation and evolution of deep-water deposits. In terraces *Ta* and *Tb*, separated by the *F1* fault zone, an extensive sheeted drift developed, bounded by the fields of cold-water corals and structural features (Figs. 3a, 4c and 4d, 8). This suggests a spread-out water mass flowing through the gentle and smooth seafloor (Figs. 2a and b, 3). In the northern limit of *Tb*, mounded drifts are locally observed with a moat developing adjacent to a high related to the *F1* fault zone (Fig. 4). The interaction of the relief with the currents' circulation causes the local enhancement of flow velocity (Faugères and Stow, 2008; Duarte et al., 2022). The contourite terrace *Tc* shows a different evolution, being smaller than the other terraces and bounded by *F2* to the south and *F4* to the north (Figs. 2a and 8). Here, contourite drifts show sheeted to mounded geometries (Figs. 5 and 8), related to its rougher topography (influence of the structural features, but also coral mounds, Fig. 5b) that locally constrained bottom-current circulation, leading to its acceleration (Faugères and Stow, 2008). The contrast between terraces *Ta–Tb* and *Tc* suggested a greater influence of tectonic activity in the sedimentary processes of the southern part of the study area, whereas oceanographic processes are dominant in the evolution of terraces *Ta* and *Tb*.

Moreover, the secondary mounded contourite deposits formed at the base of *F2*, *F4* and *F3* fault scarps, with erosional features associated with this type of drift, developed adjacent to the fault relief (Figs. 4c, d, 5b, c, 8). This reveals the constriction of the bottom-currents by the structural reliefs (Figs. 4, 5 and 8), leading to the enhancement of flow velocity (Faugères and Stow, 2008; Duarte et al., 2022). Consequently, erosional processes increase along the foot of the structure, forming contourite moats, and favouring the development of drifts with mounded geometries laterally (Faugères and Stow, 2008; Duarte et al., 2022). In areas where two fault scarps limit a small (*F3* and *F4*, >4 km) seafloor area, confined mounded drifts were observed (Figs. 5c and 8). Confined drifts are typical of morpho-structural active regions, developing in small, tectonically active basins (Faugères et al., 1999; Faugères and Stow,

2008). This further suggests the higher degree of tectonic activity in this part of the study area.

5.3. Coral mounds and oceanographic circulation

Several occurrences of cold-water corals were recognised in the study area: buried corals (echo-type *IIIB*, Fig. 6 and Table 2), partially buried (echo-type *IIC*, Fig. 6 and Table 2) and exposed at the seafloor (echo-type *IIB*, Fig. 6 and Table 2), with the latter mostly observed in the deeper coral field (Fig. 2a, d, 8). These features are part of the Atlantic Moroccan Coral Province (Fig. 1b; Hebbeln et al., 2019; Vandorpe et al., 2017). The coral fields are observed in areas of higher slope gradients (Fig. 2a and b), in the flanks of contourite terraces *Ta* and *Tb* or fault zones.

Cold-water coral mounds are known to develop in areas of vigorous bottom-current activity, as the currents transport food particles that maintain coral growth and sediment essential for mound growth (Hebbeln et al., 2016; Steinmann et al., 2020 and references therein). Some coral mounds develop near contourite moats (Figs. 4d and 5b), suggesting that these features developed in areas with enhanced current velocities. Furthermore, the occurrence of several levels of buried and exposed coral mounds (Fig. 4d–Table 2) imply various periods of mound development and aggradation, and consequently the action of an intermittent but energetic water masses circulation in the late Quaternary.

At the Present-day, the cold-water corals are known to be nearly extinct in this area and only sporadically living corals are observed (Van Rooij et al., 2011; Hebbeln et al., 2016; Vandorpe et al., 2017; Menapace et al., 2021). Therefore, these features are a relic of an oceanographic circulation system with distinctive characteristics. Wienberg et al. (2010) and Vandorpe et al. (2017, 2023) studied the age of the corals and coral mounds of the Atlantic Moroccan Coral Province, with most features having ages that correspond to glacial periods. Thus, climate changes influencing the ocean temperatures and currents circulation are an important factor in coral development. During glacial periods, the currents acting in the study area were probably more vigorous, increasing food and sediment supply, and there was an increased input in aeolian dust (Wienberg et al., 2010).

Additionally, it is possible to observe active water currents interaction with the Present-day seafloor and consequently with the cold-water coral fields. In the deeper field, most corals are exposed despite not showing evidence of new major episodes of colonization and growth (Figs. 2a, 3 and 4, 5; Wienberg et al., 2009; Vandorpe et al., 2017). This suggests the persistent circulation of a strong current, which disfavours sedimentation in this area. In the shallower field, a different setting is observed with most corals being partially buried or totally covered by ~2 m–~30 m of sediments (Figs. 2a, 4d and 5a, Table 2). The influence of weak currents could favour sedimentation, and thus causing the burial of the cold-water corals (Steinmann et al., 2020 and references therein). Furthermore, most of the shallower field developed with an ENE-WSW orientation, on top of one of the major strike-slip faults in the study area (Fig. 2a and b). The pull-apart basins associated with these faults do not show their characteristic sigmoid shape (as observed in the northernmost part of *F4*, Fig. 2a), but a more rounded form. This could result from the interaction of positive relief corals with the bottom-currents in the area, generating eddies that erode the sediments around the coral ridges.

5.4. Oceanographic implications

Bottom-current circulation influence in the study area is demonstrated by several contourite features recognised as well as by the sediment waves and coral mounds (Figs. 2–5, 8). The study area (108–1153 m water depths; Figs. 1c and 2a) is situated within the area of influence of the Eastern North Atlantic Central Water (ENACW), between 200 and 500 m water depths and the modified Antarctic

Intermediate Water (mAAIW), from 600 to >1200 m water depths (Figs. 1a, 7 and 9). Between water depths of 500 and 600 m, occurs the transitional layer between the two water masses that are mixed in this area, as previously recognised by Van Rooij et al. (2011) and Vandorpe et al. (2014, 2016). The Mediterranean Outflow Water (MOW) is also recognised, at water depths below 800 m (Figs. 7 and 9).

The recognition of contourite terraces (see section 6.2), is a good indicator that the study area has been shaped under the influence of a transitional zone between two water masses (Preu et al., 2013; Hernández-Molina et al., 2009, 2018). Presently, a mixing of ENACW and mAAIW is expected between water depths of ~600–700 m (Mienis et al., 2012; Vandorpe et al., 2016, 2023, Fig. 9). This process is also responsible for the formation of the NNE-SSW-elongated sediment waves observed along upper middle slope (Figs. 2a and b, 8; Hopfauf et al., 2001; Hernández-Molina et al., 2016b). These features indicate the action of an approximate WNW-ESE-oriented low-velocity flow, perpendicular to the waves crest. Internal tides were previously observed on the Gemini mud volcano and in the Pen Duick Escarpment (Mienis et al., 2012, Fig. 1b) and the interface between the ENACW and the AAIW is known to influence the development of the Pen Duick and Fuiza drifts (e.g., Vandorpe et al., 2023, Figs. 1b and 8). The occurrence of internal waves has been linked to the initiation and maintenance of cold-water coral mounds by previous works (Wang et al., 2019; Wienberg et al., 2018, 2020; Steinmann et al., 2020; van der Kaaden et al., 2021), as they increase the vertical transport of organic matter towards the deep-waters and sediment re-suspension (Mienis et al., 2009; Mohn et al., 2014).

Furthermore, for the mounded and confined drifts developed in the southern part of the study area it is possible to infer bottom-currents direction (Figs. 5b and c, 8). In the Northern Hemisphere, due to the Coriolis effect, the deposits developed or reworked by oceanographic currents are accumulated to the left of the current flow pathways (Faugères et al., 1999; Faugères and Stow, 2008; Llave et al., 2001). Thus, based on the geometries of the drifts and moats their north flank (Figs. 5 and 8), a local north-western directed bottom-current is suggested as the responsible for their formation. The current is deflected by morpho-structural reliefs, e.g., the SWIM lineaments (Figs. 5 and 8), with current flowing parallel to the fault reliefs (Fig. 8).

Given that the recognised coral mounds are currently inactive (see 6.3), and a cyclicity of erosional and depositional periods shaped the contourite features (see 6.2, Figs. 3–5), it is possible to infer that the margin evolution during the late Quaternary was marked by the spatially shifting of these water masses and its interface zone (Fig. 9). These changes are possibly driven by climatic variations, with interglacial periods showing similar characteristics to the present-day oceanographic circulation and the mAAIW having an even more important role during glacial periods (Fig. 9, Gu et al., 2017; Roque et al., 2019). Therefore, during glacial periods the interface shifted upward and the mAAIW circulation intensified on the study area, creating the erosional discontinuities observed in the seismic record (Figs. 3 and 9) and providing ideal conditions for the coral mound growth. During interglacial periods (such as at the Present-day), the interface is located further down and depositional processes dominate, as evidenced by the plastered sheeted drift and sediment waves observed at the seafloor (Figs. 2a and b, 3, 8) and by the burial and death of the cold-water corals (Figs. 4 and 5). In the southern region of the study area, a MOW core circulates below water depths of 800 m (Figs. 7 and 9), influencing the formation of the mounded and confined drifts, together with the mAAIW that interacts with the seafloor during glacial periods (Fig. 9).

6. Conclusions

The key findings of this study can be summarised as:

– The morpho-sedimentary evolution of the NW Moroccan Margin during the late Quaternary has been controlled by the interplay
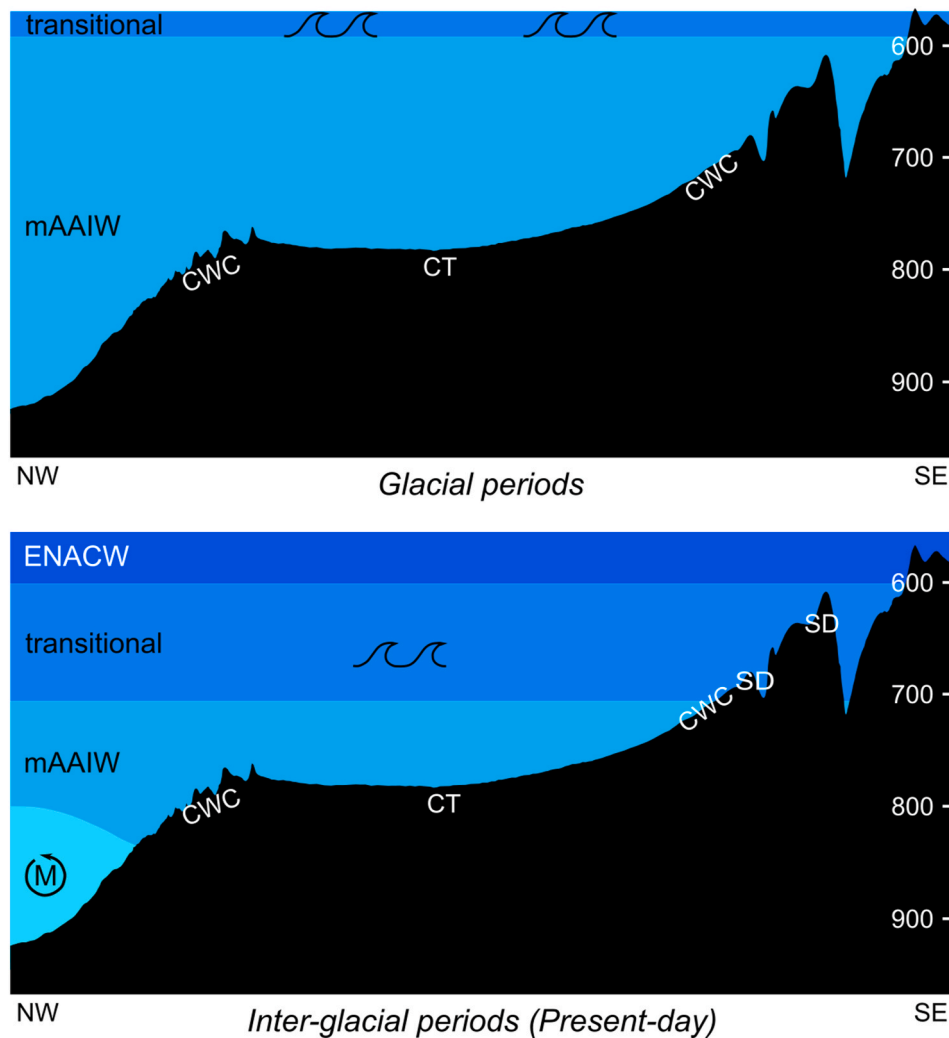
Fig. 9. Sketch of the water masses depth distribution during glacial and inter-glacial (Present-day) periods (water depth information from Gu et al., 2017; Roque et al., 2019). ENACW: Eastern North Atlantic Central Water, mAAIW: modified Antarctic Intermediate Water, M: Mediterranean Outflow Water meddies. CWC: Cold-water coral fields, CT: Contourite Terrace, SD: Sediment waves.

between active tectonics and climatic/oceanographic variations. The dominant action of each of these factors was responsible for shaping distinct parts of the study area: *i)* where oceanographic/climatic changes are the prevalent factor, contourite terraces developed with the main control being the changes in bottom-currents circulation, while *ii)* when the major control on margin evolution is tectonic activity, fault scarps confine small depocentres resulting in the formation of mounded and confined contourite drifts and local mass transport deposits.

- Structural features (e.g., strike-slip faults and mud volcanoes) have a major influence on the evolution of seafloor morphology and, consequently on the development and evolution of the sedimentary deposits in the study area. On the Moroccan Margin, the impact of these structures on sedimentary control can be observed in a short-time period (>0.9 Ma).

- Newly discovered contourite terraces, plastered sheeted, mounded and confined mounded contourite drifts and a field of sediment waves were described in the NW Moroccan Margin. These features form a well-developed contourite depositional system.

- The contourite mounded and confined drifts have been formed due to the interaction of the MOW and the mAAIW with the morpho-structure of the seafloor. Furthermore, the presence of contourite terraces and a big field of cold-water corals demonstrate the action of

internal waves due to the interaction of the ENACW with the deeper mAIW in a transitional zone.

- Two fields of coral mounds were recognised in the study area. These features developed during glacial periods when the interface zone between mAAIW and ENACW was higher than in the Present-day and the nutrient-rich mAAIW was more influential in the oceanographic re setting.

CRediT authorship contribution statement

Débora Duarte: Conceptualization, Investigation, Methodology, Writing – original draft, Writing – review & editing. **Vitor Hugo Magalhães:** Methodology, Supervision, Writing – review & editing. **F. Javier Hernández-Molina:** Investigation, Supervision, Writing – review & editing. **Cristina Roque:** Investigation, Supervision, Writing – review & editing. **Walter Menapace:** Data curation, Investigation, Writing – review & editing.

Declaration of competing interest

Data availability

The authors do not have permission to share data.

Acknowledgements

Appendix A. Supplementary data

Supplementary data to this article can be found online at https://doi. org/10.1016/j.dsr.2024.104330.

References

Ambar, I., Howe, M.R., 1979a. Observations of the Mediterranean outflow — I: mixing in the Mediterranean outflow. Deep-Sea Res. 26A, 535–554. https://doi.org/10.1016/0198-0149(79)90095-5.

Ambar, I., Howe, M.R., 1979b. Observations of the Mediterranean outflow — II: the deep circulation in the vicinity of the Gulf of Cadiz. Deep-Sea Res. 26A, 555–568. https://doi.org/10.1016/0198-0149(79)90096-7.

Ambar, I., Serra, N., Neves, F., Ferreira, T., 2008. Observations of the Mediterranean undercurrent and eddies in the gulf of cádiz during 2001. J. Mar. Syst. 71 (1–2), 195–220. https://doi.org/10.1016/j.jmarsys.2007.07.003.

Artoni, A., Rizzini, F., Roveri, M., Gennari, R., Manzi, V., Papani, G., Bernini, M., 2007. Tectonic and climatic controls on sedimentation in late Miocene cortemaggiore wedge-top basin (northwestern apennines, Italy). In: Lacombe, O., Lavé, J., Roure, F., Vergés, J. (Eds.), Thrust Belts and Foreland Basins: from Fold Kinematics to Hydrocarbon Systems. Springer, Berlin, pp. 431–456.

Bailey, W.S., McArthur, A.D., McCaffrey, W.D., 2021. Distribution of contourite drifts on convergent margins: examples from the Hikurangi subduction margin of New Zealand. Sedimentology 294–323. https://doi.org/10.1111/sed.12779.

Baringer, M.O., Price, J.F., 1999. A review of the physical oceanography of the Mediterranean outflow. Mar. Geol. 155 (1–2), 63–82. https://doi.org/10.1016/S0025-3227(98)00041-8.

Cabral, J., Mendes, V.B., Figueiredo, P., Silveira, A.B. da, Pagarete, J., Ribeiro, A., Dias, R., Ressurreição, R., 2017. Active tectonics in Southern Portugal (SW Iberia) inferred from GPS data. Implications on the regional geodynamics. J. Geodyn. 112, 1–11. https://doi.org/10.1016/j.jog.2017.10.002.

Capella, W., Hernández-Molina, F.J., Flecker, R., Hilgen, F.J., Hssain, M., Kouwenhoven, T.J., van Oorschot, M., Sierro, F.J., Stow, D.A.V., Trabucho-Alexandre, J., Tulbure, M.A., de Weger, W., Yousfi, M.Z., Krijgsman, W., 2017. Sandy contourite drift in the late Miocene Rifian Corridor (Morocco): reconstruction of depositional environments in a foreland-basin seaway. Sediment. Geol. 355, 31–57. https://doi.org/10.1016/j.sedgeo.2017.04.004.

Catuneanu, O., Abreu, V., Bhattacharya, J.P., Blum, M.D., Dalrymple, R.W., Eriksson, P. G., Fielding, C.R., Fisher, W.L., Galloway, W.E., Gibling, M.R., Giles, K.A.,

Holbrook, J.M., Jordan, R., Kendall, C.G. St C., Macurda, B., Martinsen, O.J., Miall, A.D., Neal, J.E., Nummedal, D., Pomar, L., Posamentier, H.W., Pratt, B.R., Sarg, J.F., Shanley, K.W., Steel, R.J., Strasser, A., Tucker, M.E., Winker, C., 2009. Towards the standardization of sequence stratigraphy. Earth Sci. Rev. 92, 1–33. https://doi.org/10.1016/j.earscirev.2008.10.003.

Chen, H., Zhang, W., Xie, X., Gao, Y., Liu, S., Ren, J., Wang, D., Su, M., 2022. Linking oceanographic processes to contourite features: numerical modelling of currents influencing a contourite depositional system on the northern South China Sea margin. Mar. Geol. 444, 106714 https://doi.org/10.1016/j.margeo.2021.106714.

Cunha, T.A., Matias, L.M., Terrinha, P., Negredo, A.M., Rosas, F., Fernandes, R.M.S., Pinheiro, L.M., 2012. Neotectonics of the SW Iberia margin, Gulf of Cadiz and Alboran Sea: a reassessment including recent structural, seismic and geodetic data. Geophys. J. Int. 188, 850–872. https://doi.org/10.1111/j.1365-246X.2011.05328.x.

Damuth, J.E., 1980. Use of high-frequency (3.5–12 kHz) echograms in the study of near-bottom sedimentation processes in the deep-sea: a review. Mar. Geol. 38, 51–75. https://doi.org/10.1016/0025-3227(80)90051-1.

Damuth, J.E., Hayes, D.E., 1977. Echo character of the east Brazilian continental margin and its relationship to sedimentary processes. Mar. Geol. 24, 73–95. https://doi.org/10.1016/0025-3227(77)90002-0.

de Weger, W., Hernández-Molina, F.J., Flecker, R., Sierro, F.J., Chiarella, D., Krijgsman, W., Manar, M.A., 2020. Late Miocene contourite channel system reveals intermittent overflow behavior. Geology 48 (1), 1194–1199. https://doi.org/10.1130/g47944.

Droz, L., Kergoat, R., Cochonat, P., Berné, S., 2001. Recent sedimentary events in the western gulf of lions (western mediterranean). Mar. Geol. 176, 23–37. https://doi.org/10.1016/S0025-3227(01)00147-5.

Dorschel, B., Hebbeln, D., Rüggeberg, A., Dullo, C., Freiwald, C., 2005. Growth and erosion of a cold-water coral covered carbonate mound in the Northeast Atlantic during the Late Pleistocene and Holocene. Earth Planet Sci. Lett. 233 (2005), 33–44. https://doi.org/10.1016/j.epsl.2005.01.035.

Duarte, D., Ng, Z.L., Hernández-Molina, F.J., Roque, C., Magalhães, V.H., de Weger, W., 2019. Diapirism in the Betic-Rif Foreland: The Wedge-Top Basins of the SW Iberian and NW Moroccan Margins. Preliminary results. Abstract book of Salt Tectonics: Understanding Rocks that Flow. The Geological Society of London, 29 - 31 October.

Duarte, D., Roque, C., Ng, Z.L., Hernández-Molina, F.J., Magalhães, V.H., Silva, S., Llave, E., 2022. Structural control and tectono-sedimentary evolution of the Gulf of Cadiz, SW Iberia since the late Miocene: implications for contourite depositional system. Mar. Geol. 106818 https://doi.org/10.1016/j.margeo.2022.106818.

Duarte, J.C., Rosas, F.M., Terrinha, P., Schellart, W.P., Boutelier, D., Gutscher, M.A., Ribeiro, A., 2013. Are subduction zones invading the atlantic? Evidence from the southwest iberia margin. Geology 41, 839–842. https://doi.org/10.1130/G34100.1.

EMODnet Bathymetry Consortium, 2018. EMODnet Digital Bathymetry (DTM 2018). https://doi.org/10.12770/18ff0d48-b203-4a65-94a9-5fd8b0ec35f6 [WWW Document].

Faugères, J.C., Stow, D.A.V., Imbert, P., Viana, A., 1999. Seismic features diagnostic of contourite drifts. Mar. Geol. 162 (1), 1–36. https://doi.org/10.1016/S0025-3227(99)00068-7.

Faugères, J., Stow, D., 2008. Contourite drifts. Nature, evolution and controls. In: Rebesco, M., Camerlenghi, A. (Eds.), Contourites. Developments in Sedimentology, vol. 60, pp. 259–288. https://doi.org/10.1016/S0070-4571(08)10014-0.

Flecker, R., Krijgsman, W., Capella, W., de Castro Martíns, C., Dmitrieva, E., Mayser, J.P., Marzocchi, A., Modestu, S., Ochoa, D., Simon, D., Tulbure, M., van den Berg, B., van der Schee, M., de Lange, G., Ellam, R., Govers, R., Gutjahr, M., Hilgen, F., Kouwenhoven, T., Lofi, J., Meijer, P., Sierro, F.J., Bachiri, N., Barhoun, N., Alami, A. C., Chacon, B., Flores, J.A., Gregory, J., Howard, J., Lunt, D., Ochoa, M., Pancost, R., Vincent, S., Yousfi, M.Z., 2015. Evolution of the Late Miocene Mediterranean-Atlantic gateways and their impact on regional and global environmental change. Earth Sci. Rev. 150, 365–392. https://doi.org/10.1016/j.earscirev.2015.08.007.

Flinch, J.F., Soto, J.I., 2017. Allochthonous triassic and salt tectonic processes in the betic-rif orogenic arc. In: Soto, J.I., Flinch, J.F., Tari, G. (Eds.), Permo-Triassic Salt Provinces of Europe, North Africa and the Atlantic Margins. Elsevier, pp. 417–446. https://doi.org/10.1016/B978-0-12-809417-4.00020-3.

Gamboa, D., Omira, R., Piedade, A., Terrinha, P., Roque, C., Zitellini, N., 2021. Destructive episodes and morphological rejuvenation during the lifecycles of tectonically active seamounts: Insights from the Gorringe Bank in the NE Atlantic. Earth Planet. Sci. Lett. 559, 116772. https://doi.org/10.1016/j.epsl.2021.116772.

García, M., Hernández-Molina, F.J., Llave, E., Stow, D.A.V., León, R., Fernández-Puga, M. C., Diaz del Río, V., Somoza, L., 2009. Contourite erosive features caused by the mediterranean outflow water in the gulf of Cadiz: quaternary tectonic and oceanographic implications. Mar. Geol. 257, 24–40. https://doi.org/10.1016/j.margeo.2008.10.009.

García, M., Llave, E., Hernández-Molina, F.J., Lobo, F.J., Ercilla, G., Alonso, B., Casas, D., Mena, A., Fernández-Salas, L.M., 2020. The role of late Quaternary tectonic activity and sea-level changes on sedimentary processes interaction in the Gulf of Cadiz upper and middle continental slope (SW Iberia). Mar. Petrol. Geol. 121, 104595 https://doi.org/10.1016/j.marpetgeo.2020.104595.

Gardner, J.M., 2001. Mud volcanoes revealed and sampled on the Western Moroccan continental margin. Geophys. Res. Lett. 28 (2), 339–342. https://doi.org/10.1029/2000GL012141.

Gu, S., Liu, Z., Zhang, J., Rempfer, J., Joos, F., Opp, D.W., 2017. Coherent response of antarctic intermediate water and atlantic meridional overturning circulation during the last deglaciation: reconciling contrasting neodymium isotope reconstructions from the tropical atlantic. Paleoceanography 32, 1036–1053. https://doi.org/10.1002/2017PA003092.

Gutscher, M.-A., Malod, J., Rehault, J.-P., Contrucci, I., Klingelhoefer, F., Mendes-Victor, L., Spakman, W., 2002. Evidence for active subduction beneath Gibraltar.

Geology 30 (12), 1071–1074. https://doi.org/10.1130/0091-7613(2002) 030<1071:EFASBG>2.0.CO;2.

Gutscher, M.A., Dominguez, S., Westbrook, G.K., Gente, P., Babonneau, N., Mulder, T., Gonthier, E., Bartolome, R., Luis, J., Rosas, F., Terrinha, P., 2009. Tectonic shortening and gravitational spreading in the Gulf of Cadiz accretionary wedge: observations from multi-beam bathymetry and seismic profiling. Mar. Petrol. Geol. 26, 647–659. https://doi.org/10.1016/j.marpetgeo.2007.11.008.

Hebbeln, D., Van Rooij, D., Wienberg, C., 2016. Good neighbours shaped by vigorous currents: cold-water coral mounds and contourites in the North Atlantic. Mar. Geol. 378, 114–126. https://doi.org/10.1016/j.margeo.2016.01.014.

Hebbeln, D., Bender, M., Gaide, S., Titschack, J., Vandorpe, T., Van Rooij, D., Wintersteller, P., Wienberg, C., 2019. Thousands of cold-water coral mounds along the Moroccan Atlantic continental margin: distribution and morphometry. Mar. Geol. 411, 51–61. https://doi.org/10.1016/j.margeo.2019.02.001.

Hensen, C., Scholz, F., Nuzzo, M., Valadares, V., Gràcia, E., Terrinha, P., Liebetrau, V., Kaul, N., Silva, S., Martínez-Loriente, S., Bartolome, R., Piñero, E., Magalhães, V.H., Schmidt, M., Weise, S.M., Cunha, M., Hilario, A., Perea, H., Rovelli, L., Lackschewitz, K., 2015. Strike-slip faults mediate the rise of crustal-derived fluids and mud volcanism in the deep sea. Geology 43 (4), 339–342. http://doir.org/10.1130/G36359.1.

Hernández-Molina, F.J., Campbell, S., Badalini, G., Thompson, P., Walker, R., Soto, M., Conti, B., Preu, B.Thiéblemont, Hyslop, L., Miramontes, E., Morales, E., 2018. Large bedforms on contourite terraces: sedimentary and conceptual implications. Geology 46 (1), 27–30. https://doi.org/10.1130/G39655.1.

Hernández-Molina, F.J., Llave, E., Somoza, L., Fernández-Puga, M.C., Maestro, A., León, R., Medialdea, T., Barnolas, A., García, M., Díaz del Río, V., Fernández-Salas, L. M., Vázquez, J.T., Lobo, F., Alveirinho Dias, J.M., Rodero, J., Gardner, J., 2003. Looking for clues to paleoceanographic imprints: a diagnosis of the Gulf of Cadiz contourite depositional systems. Geology 31, 19–22. https://doi.org/10.1130/0091-7613(2003)031<0019:LFCTPI>2.0.CO;2.

Hernández-Molina, F.J., Paterlini, M., Violante, R., Marshall, P., de Isasi, M., Somoza, L., Rebesco, M., 2009. Contourite depositional system on the Argentine Slope: An exceptional record of the influence of Antarctic water masses. Geology 37 (6), 507–510. https://doi.org/10.1130/G25578A.1.

Hernández-Molina, F.J., Serra, N., Stow, D.A.V., Llave, E., Ercilla, G., van Rooij, D., 2011. Along-slope oceanographic processes and sedimentary products around the Iberian margin. Geo-Marine Lett. 31, 315–341. https://doi.org/10.1007/s00367-011-0242-2.

Hernández-Molina, F.J., Sierro, F.J., Llave, E., Roque, C., Stow, D.A.V., Williams, T., Lofi, J., Van der Schee, M., Arnáiz, A., Ledesma, S., Rosales, C., Rodríguez-Tovar, F. J., Pardo-Igúzquiza, E., Brackenridge, R.E., 2016a. Evolution of the gulf of Cadiz margin and southwest Portugal contourite depositional system: tectonic, sedimentary and paleoceanographic implications from IODP expedition 339. Mar. Geol. 377, 7–39. https://doi.org/10.1016/j.margeo.2015.09.013.

Hernández-Molina, F.J., Stow, D.A.V., Alvarez-Zarikian, C.A., Acton, G., Bahr, A., Balestra, B., Ducassou, E., Flood, R., Flores, J.-A., Furota, S., Grunert, P., Hodell, D., Jimenez-Espejo, F., Kim, J.K., Krissek, L., Roque, C., Pereira, H., Fernanda, M., Goñi, S., Sierro, F.J., Singh, A.D., Sloss, C., Takashimizu, Y., Tzanova, A., Voelker, A., Williams, T., Xuan, C., 2014. Onset of mediterranean outflow into the north Atlantic. Science 344 (80), 1244–1250. https://doi.org/10.1126/science.1251306, 2014.

Hernández-Molina, F.J., Wåhlin, A., Bruno, M., Ercilla, E., Llave, E., Serra, N., Rosón, G., Puig, P., Rebesco, M., Van Rooij, D., Roque, D., González-Pola, C., Sánchez, F., Gómez, M., Preu, B., Schwenk, T., Hanebuth, T.J.J., Sánchez Leal, R.F., García-Lafuente, J., Brackenridge, R.E., Juan, C., Stow, D.A.V., Sánchez-González, J.M., 2016b. Oceanographic processes and morphosedimentary products along the Iberian margins: a new multidisciplinary approach. Mar. Geol. 378, 127–156. https://doi.org/10.1016/j.margeo.2015.12.0080205-32.

Hopfauf, V., Spieß, V., Geowissenschaften, F., 2001. A three-dimensional theory for the development and migration of deep sea sedimentary waves. Deep Sea Res. Oceanogr. Res. Pap. 48 (11), 2497–2519. https://doi.org/10.1016/S0967-0637(01)00026-7.

Hüpers, A., Menapace, W., Magalhaes, V., Kopf, A., the M149 scientific party, 2019. Expedition M149 with R/V Meteor Cruise Report. Las Palmas (Canary Island, Spain) – Cadiz (Spain) 24.07.2018 – 24.08.2018. MARUM Cruise Report. MARUM– Center for Marine Environmental Sciences, Bremen, Germany.

Iribarren, L., Vergés, J., Camurri, F., Fullea, J., Fernàndez, M., 2007. The structure of the atlantic-mediterranean transition zone from the alboran sea to the horseshoe abyssal plain (Iberia-Africa plate boundary). Mar. Geol. 243, 97–119. https://doi.org/10.1016/j.margeo.2007.05.011.

Ivanov, M.K., Kenyon, N., Nielsen, T., Wheeler, A., Monteiro, H., Gardner, J., Comas, M., Akhmanov, A., Akhmetzhanov, G., 2000. Goals and principal results of the TTR-9 cruise. IOC/UNESCO Work. Rep. 168, 3–4.

Kirby, A., Hernández-Molina, F.J., Rodriguez, P., Conti, B., 2021. Sedimentary stacking pattern of plastered drifts: an example from the Cenozoic on the Uruguayan continental slope. Mar. Geol. 440, 106567 https://doi.org/10.1016/j.margeo.2021.106567.

Krijgsman, W., Capella, W., Simon, D., Hilgen, F.J., Kouwenhoven, T.J., Meijer, P.T., Sierro, F.J., Tulbure, M.A., van den Berg, Bas C.J., van der Schee, M., Flecker, R., van der Berg, B.C.J., van der Schee, M., Flecker, R., 2018. The Gibraltar corridor: watergate of the messinian salinity Crisis. Mar. Geol. 403, 238–246. https://doi.org/10.1016/j.margeo.2018.06.008.

Kuhn, G., Weber, M.E., 1993. Acoustical characterization of sediments by Parasound and 3.5 kHz systems: related sedimentary processes on the southeastern Weddell Sea continental slope. Antarctica. Mar. Geol. 113, 201–217. https://doi.org/10.1016/0025-3227(93)90018-Q.

Lebreiro, S.M., Antón, L., Reguera, M.I., Marzocchi, A., 2018. Paleoceanographic and climatic implications of a new Mediterranean Outflow branch in the southern Gulf of Cadiz. Quat. Sci. Rev. 197, 92–111. https://doi.org/10.1016/j.quascirev.2018.07.036.

Leeder, M.R., 2011. Tectonic sedimentology: sediment systems deciphering 848 global to local tectonics. Sedimentology 58, 2–56. https://doi.org/10.1111/j.1365-3091.2010.01207.x.

León, R., Somoza, L., Medialdea, T., Hernández-Molina, F.J., Vázquez, J.T., Díaz-del-Rio, V., González, F.J., 2010. Pockmarks, collapses and blind valleys in the Gulf of Cádiz. Geo Mar. Lett. 30, 231–247. https://doi.org/10.1007/s00367-009-0169-z.

León, R., Somoza, L., Medialdea, T., Vázquez, J.T., González, F.J., López-González, N., Casas, D., Mata, M.P., Fernández-Puga, M.C., Giménez-Moreno, C.J., Díaz del-Río, V., 2012. New discoveries of mud volcanoes on the Moroccan Atlantic continental margin (Gulf of Cádiz): morphostructural characterization. Geo Mar. Lett. 32, 473–488. https://doi.org/10.1007/s00367-012-0275-1.

Liu, S., Hernández-Molina, F.J., Lei, Z., Duarte, D., Chen, H., Wang, C., Lei, Y., Zhuo, H., Huang, S., Zhang, L., Su, M., 2021. Fault-controlled contourite drifts in the southern South China Sea: tectonic, oceanographic, and conceptual implications. Mar. Geol. 433 https://doi.org/10.1016/j.margeo.2021.106420.

Liu, S., Van Rooij, D.V., Vandorpe, T., González-Pola, C., Ercilla, G., Hernández-Molina, F.J., 2019. Morphological features and associated bottom-current dynamics in the Le Danois Bank region (southern Bay of Biscay, NE Atlantic): a model in atopographically constrained small basin. Deep-Sea Res. Part I 149. https://doi.org/10.1016/j.dsr.2019.05.014.

Llave, E., Hernández-Molina, F.J., García, M., Ercilla, G., Roque, C., Juan, C., Mena, A., Preu, B., Rooij, D. Van, Rebesco, M., Brackenridge, R., Jané, G., Gómez-ballesteros, M., Stow, D., 2019. Contourites along the Iberian continental margins: conceptual and economic implications. Geol. Soc. London, Spec. Publ. 476, 403–436.

Llave, E., Hernández-Molina, F.J., Somoza, L., Díaz del Río, V., Stow, D.A.V., Maestro, A., Alveirinho Dias, J.M., 2001. Seismic stacking pattern of the Faro-Albufeira contourite system (Gulf of Cadiz): a Quaternary record of paleoceanographic and tectonic influences. Mar. Geophys. Res. 22, 487–508. https://doi.org/10.1023/A:1016355801344.

Llave, E., Hernández-Molina, F.J., Somoza, L., Stow, D.A., Díaz del Río, V., Mar, D.C., Vigo, U. De, Southampton, S., 2007a. Quaternary evolution of the contourite depositional system in the Gulf of Cadiz. Geol. Soc. Spec. Publ. 276, 49–79. https://doi.org/10.1144/GSL.SP.2007.276.01.03.

Llave, E., Hernández-Molina, F.J., Stow, D.A.V., Fernández-Puga, M.C., García, M., Vázquez, J.T., Maestro, A., Somoza, L., Díaz del Río, V., 2007b. Reconstructions of the Mediterranean Outflow Water during the Quaternary based on the study of changes in buried mounded drift stacking pattern in the Gulf of Cadiz. Mar. Geophys. Res. 28, 379–394. https://doi.org/10.1007/s11001-007-9040-7.

Llave, E., Schönfeld, J., Hernández-Molina, F.J., Mulder, T., Somoza, L., Díaz Del Río, V., Sánchez-Almazo, I., 2006. High-resolution stratigraphy of the Mediterranean outflow contourite system in the Gulf of Cadiz during the late Pleistocene: The impact of Heinrich events. Mar. Geol. 227, 241–262. https://doi.org/10.1016/j.margeo.2005.11.015.

Louarn, E., Morin, P., 2011. Antarctic intermediate water influence on Mediterranean Sea water outflow. Deep Sea Res. Oceanogr. Res. Pap. 56, 932–942. https://doi.org/10.1016/j.dsr.2011.05.009.

Lozano, P., Fernández-Salas, L.M., Hernández-Molina, F.J., Sánchez-Leal, R., Sánchez-Guillamón, O., Palomino, D., Farias, C., Mateo-Ramírez, Á., López-González, N., García, M., Vázquez, J.-T., Vila, Y., Rueda, J.L., 2020. Multiprocess interaction shaping geoforms and controlling substrate types and benthic community distribution in the Gulf of Cádiz. Mar. Geol. 423, 106139 https://doi.org/10.1016/j.margeo.2020.106139.

Maestro, A., Somoza, L., Medialdea, T., Talbot, C.J., Lowrie, A., Vázquez, J.T., Díaz-del-Río, V., 2003. Large-scale slope failure involving triassic and middle Miocene salt and shale in the gulf of Cadiz (Atlantic Iberian margin). Terra. Nova 15, 380–391. https://doi.org/10.1046/j.1365-3121.2003.00513.x.

Magalhães, V.H., Buffett, B., Archer, D., McGuire, P., Pinheiro, L.M., Gardner, J.M., 2019. Effects of oceanographic changes on controlling the stability of gas hydrates and the formation of authigenic carbonates at mud volcanoes and seepage sites on the Iberian margin of the Gulf of Cadiz. Mar. Geol. 412, 69–80. https://doi.org/10.1016/j.margeo.2019.03.002.

Maldonado, A., Somoza, L., Pallarés, L., 1999. The betic orogen and the Iberian-African boundary in the gulf of Cadiz: geological evolution (central North Atlantic). Mar. Geol. 155, 9–43. https://doi.org/10.1016/S0025-3227(98)00139-X.

Matias, H., Kress, P., Terrinha, P., Mohriak, W., Menezes, P.T.L., Matias, L., Santos, F., Sandnes, F., 2011. Salt tectonics in the western gulf of Cadiz, southwest Iberia. Am. Assoc. Petrol. Geol. Bull. 95, 1667–1698. https://doi.org/10.1306/01271110032.

Medialdea, T., Somoza, L., Pinheiro, L.M., Fernández-Puga, M.C., Vázquez, J.T., León, R., Ivanov, M.K., Magalhaes, V., Díaz-del-Río, V., Vegas, R., 2009. Tectonics and mud volcano development in the Gulf of Cádiz. Mar. Geol. 261, 48–63. https://doi.org/10.1016/j.margeo.2008.10.007.

Medialdea, T., Vegas, R., Somoza, L., Vázquez, J.T., Maldonado, A., Díaz-Del-Río, V., Maestro, A., Córdoba, D., Fernández-Puga, M.C., 2004. Structure and evolution of the "Olistostrome" complex of the Gibraltar Arc in the Gulf of Cádiz (eastern Central Atlantic): evidence from two long seismic cross sections. Mar. Geol. 209, 173–198. https://doi.org/10.1016/j.margeo.2004.05.029.

Menapace, W., Chahid, D., Duarte, D., Fleischmann, T., Heitmann-Bacza, C., Kramer, L., Krupiński, S., Leymann, T., Mai, A., Morales, N., Otte, F., Schmidt, C., Tamborrino, L., Vittori, V., Xu, S., Zehnle, H., Zhang, J., 2021. Long-term Monitoring of Fluid and Solid Emissions at the African-Eurasian Tectonic Boundary in the ALBOran Sea and the Gulf of Cadiz. Cruise No. M167, ALBOCA II. MARUM – Center for Marine Environmental Sciences. University of Bremen. https://doi.org/10.48433/cr_m167.

Miall, A.D., 1985. Architectural elements and bounding surfaces in channelized clastic deposits: notes on comparisons between fluvial and turbidite systems. In: Taira, A., Masuda, F. (Eds.), Sedimentary Facies in the Active Plate Margin. Terra Scientific Publishing Company, TERRAPUB), Tokyo, pp. 3–15.

Mienis, F., de Stigter, H.C., de Haas, H., van der Land, C., Van Weering, T.C.E., 2012. Hydrodynamic conditions in a cold-water coral mound area on the Renard Ridge, southern Gulf of Cadiz. J. Mar. Syst. 96–97, 61–71. https://doi.org/10.1016/j.jmarsys.2012.02.002.

Mienis, F., de Stigter, H.C., de Haas, H., van Weering, T.C.E., 2009. Near-bed particle deposition and resuspension in a cold-water coral mound area at the Southwest Rockall Trough margin, NE Atlantic Deep. Res. Part I Oceanogr. Res. Pap. 56, 1026–1038. https://doi.org/10.1016/j.dsr.2009.01.006.

Miramontes, E., Thiéblemont, A., Babonneau, N., Penven, P., Raisson, F., Droz, L., Jorry, S.J., Fierens, R., Counts, J.W., Wilckens, H., Cattaneo, A., Jouet, G., 2021. Contourite and mixed turbidite-contourite systems in the Mozambique Channel (SW Indian Ocean): link between geometry, sediment characteristics and modelled bottom currents. Mar. Geol. 37, 106502 https://doi.org/10.1016/j.margeo.2021.106502.

Mitchum, R.M., Vail, P.R., Sangree, J.B., 1977a. Seismic stratigraphy and global changes of sea level, part 6: stratigraphic interpretation of seismic reflection patterns in depositional sequences. In: Payton, C.E. (Ed.), Seismic Stratigraphy-Applications to Hydrocarbon Exploration. American Association of Petroleum Geologists, pp. 117–133.

Mitchum, R.M., Vail, P.R., Thompson III, S., 1977b. Seismic stratigraphy and global changes of sea level, part 2: the depositional sequence as a basic unit for stratigraphic analysis. In: Payton, C.E. (Ed.), Seismic Stratigraphy-Applications to Hydrocarbon Exploration. American Association of Petroleum Geologists, pp. 53–62.

Mitchum, R.M., Vail, P.R., Thompson III, S., 1977c. Seismic stratigraphy and global changes of sea level, part 1: overview. In: Payton, C.E. (Ed.), Seismic Stratigraphy-Applications to Hydrocarbon Exploration. American Association of Petroleum Geologists, pp. 51–52.

Mohn, C., Rengstorf, A., White, M., Duineveld, G., Mienis, F., Soetaert, K., Grehan, A., 2014. Linking benthic hydrodynamics and cold-water coral occurrences: a high-resolution model study at three cold-water coral provinces in the NE Atlantic. Prog. Oceanogr. 122, 92–104. https://doi.org/10.1016/j.pocean.2013.12.003.

Mulder, T., Ducassou, E., Hanquiez, V., Principaud, M., Fauquembergue, K., Tournadour, E., Chabaud, L., Reijmer, J., Recouvreur, A., Gillet, H., Borgomano, J., Schmitt, A., Moal, P., 2019. Contour current imprints and contourite drifts in the Bahamian archipelago. Sedimentology 666 (4), 1192–1221. https://doi.org/10.1111/sed.12587.

Müller-Michaelis, A., Uenzelmann-Neben, G., Stein, R., 2013. A revised Early Miocene age for the instigation of the Eirik Drift, offshore southern Greenland: evidence from high-resolution seismic reflection data. Mar. Geol. 340, 1–15. https://doi.org/10.1016/j.margeo.2013.04.012.

Nelson, C.H., Baraza, J., Maldonado, A., Rodero, J., Escutia, C., Barber, J.H., 1999. Influence of the Atlantic inflow and Mediterranean outflow currents on late Quaternary sedimentary facies of the Gulf of Cadiz continental margin. Mar. Geol. 155, 99–129. https://doi.org/10.1016/S0025-3227(98)00143-1.

Ng, Z.L., Hernández-Molina, F.J., Duarte, D., Roque, C., Sierro, F.J., Llave, E., Manar, M., 2021a. Late Miocene contourite depositional system of the gulf of Cadiz: the sedimentary signature of the paleo-mediterranean outflow water. Mar. Geol. 442 https://doi.org/10.1016/j.margeo.2021.106605.

Ng, Z.L., Hernández-Molina, F.J., Duarte, D., Sierro, F.J., Ledesma, S.M., Rogerson, M., Llave, E., Roque, C., Manar, M.A., 2021b. Latest Miocene restriction of the mediterranean outflow water: a perspective from the gulf of cádiz. Geo Mar. Lett. 41 https://doi.org/10.1007/s00367-021-00693-9.

Nielsen, T., Knutz, P.C., Kuijpers, A., 2008. Seismic expression of contourite depositional systems. In: Rebesco, M., Camerlenghi, A. (Eds.), Contourites. Developments in Sedimentology, vol. 60, pp. 301–321. https://doi.org/10.1016/S0070-4571(08)10016-4.

Palomino, D., López-González, N., Vázquez, J.T., Fernández-Salas, L.M., Rueda, J.L., Sánchez-Leal, R., Díaz-del-Río, V., 2016. Multidisciplinary study of mud volcanoes and diapirs and their relationship to seepages and bottom currents in the Gulf of Cádiz continental slope (northeastern sector). Mar. Geol. 378, 196–212. https://doi.org/10.1016/j.margeo.2015.10.001.

Perez-Garcia, C., Berndt, C., Klaeschen, D., Mienert, J., Haffert, L., Depreiter, D., Haeckel, M., 2011. Linked halokinesis and mud volcanism at the Mercator mud volcano, Gulf of Cadiz. J. Geophys. Res. Solid Earth 116 (B5). https://doi.org/10.1029/2010JB008061.

Pinheiro, L.M., Ivanov, M., Sautkin, A.P., Akhmanov, G.G., Magalhães, V.H., Volkonskaya, A., Monteiro, H., Somoza, L., Gardner, J., Hamouni, N., Cunha, M.R.d., 2003. Mud volcanism in the gulf of Cadiz: results from the TTR-10 cruise. Mar. Geol. 195, 131–151.

Pomar, L., Morsilli, M., Hallock, P., Bádenas, B., 2012. Internal waves, an under-explored source of turbulence events in the sedimentary record. Earth Sci. Rev. 111 (1–2), 56–81. https://doi.org/10.1016/j.earscirev.2011.12.005.

Preu, B., Hernández-Molina, F.J., Violante, R., Piola, A.R., Paterlini, C.M., Schwenk, T., Voigt, I., Krastel, S., Spiess, V., 2013. Morphosedimentary and hydrographic features of the northern Argentine margin: the interplay between erosive, depositional and gravitational processes and its conceptual implications. Deep-sea Res. Part I: Oceanogr. Res. Paper. 75, 157–174. https://doi.org/10.1016/j.dsr.2012.12.013.

Ramos, A., Fernández, O., Muñoz, J.A., Terrinha, P., 2017a. Impact of basin structure and evaporite distribution on salt tectonics in the Algarve Basin, Southwest Iberian margin. Mar. Petrol. Geol. 88, 961–984. https://doi.org/10.1016/j.marpetgeo.2017.09.028.

Ramos, A., Fernández, O., Terrinha, P., Muñoz, J.A., 2017b. Neogene to recent contraction and basin inversion along the Nubia-Iberia boundary in SW Iberia. Tectonics 36, 257–286. https://doi.org/10.1002/2016TC004262.

Ramos, A., Fernández, O., Terrinha, P., Muñoz, J.A., Arnaiz, Á., 2020. Paleogeographic evolution of a segmented oblique passive margin: the case of the SW Iberian margin. Int. J. Earth Sci. 109, 1871–1895. https://doi.org/10.1007/s00531-020-01878-w.

Rebesco, M., Hernández-Molina, F.J., Van Rooij, D., Wåhlin, A., 2014. Contourites and associated sediments controlled by deep-water circulation processes: state-of-the-art and future considerations. Mar. Geol. 352, 111–154. https://doi.org/10.1016/j.margeo.2014.03.011.

Ribó, M., Durán, R., Puig, P., Van Rooij, D., Guillén, J., Masqué, P., 2018. Large sediment waves over the Gulf of Roses upper continental slope (NW Mediterranean). Mar. Geol. 399, 84–96. https://doi.org/10.1016/j.margeo.2018.02.006.

Richardson, P.L., Bower, A.S., Zenk, W., 2000. A census of Meddies tracked by floats. Prog. Oceanogr. 45, 209–250. https://doi.org/10.1016/S0079-6611(99)00053-1.

Rogerson, M., Rohling, E.J., Bigg, G.R., Ramirez, J., 2012. Paleoceanography of the Atlantic-Mediterranean exchange: overview and first quantitative assessment of climatic forcing. Verv. Geophys. 50 https://doi.org/10.1029/2011RG000376.

Roque, C., Duarte, H., Terrinha, P., Valadares, V., Noiva, J., Cachão, M., Ferreira, J., Legoinha, P., Zitellini, N., 2012. Pliocene and Quaternary depositional model of the Algarve margin contourite drifts (Gulf of Cadiz, SW Iberia): seismic architecture, tectonic control and paleoceanographic insights. Mar. Geol. 303–306, 42–62. https://doi.org/10.1016/j.margeo.2011.11.001.

Roque, D., Gomiz-Pascual, J.J., Bruno, M., Sánchez-Leal, R., González, C.J., García, M., Fernández-Salas, L.M., Hernández-Molina, F.J., 2023. Tidal dynamics on the upper continental slope of the eastern Gulf of Cádiz: the interplay between water masses and its effects on seafloor morphology. Prog. Oceanogr. 212, 102954 https://doi.org/10.1016/j.pocean.2022.102954.

Roque, D., Parras-Berrocal, I., Bruno, M., Sánchez-Leal, R., Hernández-Molina, F.J., 2019. Seasonal variability of intermediate water masses in the Gulf of Cádiz: implications of the Antarctic and subarctic seesaw. Ocean Sci. 15, 1381–1397. https://doi.org/10.5194/os-15-1381-2019.

Roque, C., Hernández-Molina, F.J., Madureira, P., Quartau, R., Magalhães, V.H., Brito, P., Vázquez, J.T., Somoza, L., 2022. Interplay of deep-marine sedimentary processes with seafloor morphology offshore Madeira Island (Central NE-Atlantic). Mar. Geol. 443, 106675 https://doi.org/10.1016/j.margeo.2021.106675.

Rosas, F.M., Duarte, J.C., Terrinha, P., Valadares, V., Matias, L., 2009. Morphotectonic characterization of major bathymetric lineaments in Gulf of Cadiz (Africa-Iberia plate boundary): insights from analogue modelling experiments. Mar. Geol. 261, 33–47. https://doi.org/10.1016/j.margeo.2008.08.002.

Sánchez-Leal, R.F., Bellanco, M.J., Fernández-Salas, L.M., García-Lafuente, J., Gasser-Rubinat, M., González-Pola, C., Hernández-Molina, F.J., Pelegrí, J.L., Peliz, A., Relvas, P., Roque, D., Ruiz-Villarreal, M., Sammartino, S., Sánchez-Garrido, J.C., 2017. The mediterranean overflow in the gulf of Cadiz: a rugged journey. Sci. Adv. 3, 1–12. https://doi.org/10.1126/sciadv.aao0609.

Schlitzer, R., 2015. Data analysis and visualization with Ocean Data View. CMOS Bullet. SCMO 43 (1), 9–13.

Serra, N., Ambar, I., Käse, R.H., 2005. Observations and numerical modelling of the Mediterranean outflow splitting and eddy generation. Deep Sea Res. Part II Top. Stud. Oceanogr. 52, 383–408. https://doi.org/10.1016/j.dsr2.2004.05.025.

Silva, S., Terrinha, P., Matias, L., Duarte, J.C., Roque, C., Ranero, C.R., et al., 2017. Micro-seismicity in the Gulf of Cadiz: is there a link between micro-seismicity, high magnitude earthquakes and active faults? Tectonophysics 717, 226–241. https://doi.org/10.1016/j.tecto.2017.07.026.

Steinmann, L., Baques, M., Wenau, S., Schwenk, T., Spiess, V., Piola, A.R., Bozzano, G., Violante, R., Kasten, S., 2020. Discovery of a giant cold-water coral mound province along the northern Argentine margin and its link to the regional Contourite Depositional System and oceanographic setting. Mar. Geol. 427, 106223 https://doi.org/10.1016/j.margeo.2020.106223.

Stich, D., Serpelloni, E., Delismancilla, F., Morales, J., 2006. Kinematics of the Iberia–Maghreb plate contact from seismic moment tensors and GPS observations. Tectonophysics 426, 295–317.

Terrinha, P., Matias, L., Vicente, J., Duarte, J., Luís, J., Pinheiro, L., Lourenço, N., Diez, S., Rosas, F., Magalhães, V., Valadares, V., Zitellini, N., Roque, C., Víctor, L.M., 2009. Morphotectonics and strain partitioning at the Iberia-Africa plate boundary from multibeam and seismic reflection data. Mar. Geol. 267, 156–174. https://doi.org/10.1016/j.margeo.2009.09.012.

Terrinha, P., Ramos, A., Neres, M., Valadares, V., Duarte, J., Martínez-Loriente, S., Silva, S., Mata, J., Kullberg, J.C., Casas-Sainz, A., Matias, L., Fernández, Ó., Muñoz, J.A., Ribeiro, C., Font, E., Neves, C., Roque, C., Rosas, F., Pinheiro, L., Bartolomé, R., Sallarès, V., Magalhães, V., Medialdea, T., Somoza, L., Gràcia, E., Hensen, C., Gutscher, M.-A., Ribeiro, A., Zitellini, N., 2019. The alpine orogeny in the west and southwest Iberia margins. In: Quesada, C., Oliveira, J.T. (Eds.), The Geology of Iberia: A Geodynamic Approach. Springer International Publishing, Switzerland, pp. 1119 487–505. https://doi.org/10.1007/978-3-030-11295-0.

van der Kaaden, A.-S., Mohn, C., Gerkema, T., Maier, S.R., de Froe, E., van de Koppel, J., Rietkerk, M., Soetaert, K., van Oevelen, D., 2021. Feedbacks between hydrodynamics and cold-water coral mound development. Deep Sea Res. Oceanogr. Res. Pap. 178, 10364 https://doi.org/10.1016/j.dsr.2021.103641.

Vandorpe, T., Delivet, S., Blamart, D., Wienberg, C., Bassinot, F., Mienis, F., Stuut, J.-B. W., Van Rooij, D., 2023. Palaeoceanography and hydrodynamic variability for the last 47 kyr in the southern Gulf of Cádiz (Atlantic Moroccan margin): sedimentary and climatic implications. Deposit. Rec. 9 (1), 30–51. https://doi.org/10.1002/dep2.212.

Vandorpe, T., Martins, I., Vitorino, J., Hebbeln, D., García, M., Van Rooij, D., 2016. Bottom currents and their influence on the sedimentation pattern in the El Arraiche

mud volcano province, southern Gulf of Cadiz. Mar. Geo. 378, 114–126. https://doi.org/10.1016/j.margeo.2015.11.012.

Vandorpe, T., Van Rooij, D., de Haas, H., 2014. Stratigraphy and paleoceanography of a topography-controlled contourite drift in the Pen Duick area, southern Gulf of Cádiz. Mar. Geo. 349, 136–151. https://doi.org/10.1016/j.margeo.2014.01.007.

Vandorpe, T., Wienberg, C., Hebbeln, D., Van den Berghe, M., Gaide, S., Wintersteller, P., Van Rooij, D., 2017. Multiple generations of buried cold-water coral mounds since the early-middle pleistocene transition in the atlantic Moroccan coral province, southern gulf of cádiz. Palaeogeogr. Palaeoclimatol. Palaeoecol. 485, 293–304. https://doi.org/10.1016/j.palaeo.2017.06.021.

Van Rensbergen, P., Depreiter, D., Pannemans, B., Moerkerke, G., Van Rooij, D., Marsset, B., Akhmanov, G., Blinova, V., Ivanov, M., Rachidi, M., Magalhaes, V., Pinheiro, L., Cunha, M., Henriet, J.-P., 2005. The El Arraiche mud volcano field at the Moroccan atlantic slope, gulf of Cadiz. Mar. Geol. 219 (1), 1–17. https://doi.org/10.1016/j.margeo.2005.04.007.

Van Rensbergen, P., Hillis, R.R., Maltman, J., Morley, C.K., 2003. In: Van Rensbergen, P., Hillis, R.R., Maltman, J., Morley, C.K. (Eds.), Subsurface Sediment Mobilization, Subsurface Sediment Mobilisation, vol. 216. Special Publication of the Geological Society of London, pp. 1–8.

Van Rooij, D., Blamart, D., De Mol, L., Mienis, F., Pirlet, H., Wehrmann, L.M., Barbieri, R., Maignien, L., Templer, S.P., de Haas, H., Hebbeln, D., Frank, N., Larmagnat, S., Stadnitskaia, A., Stivaletta, N., van Weering, T., Zhang, Y., Hamoumi, N., Cnudde, V., Duyck, P., Henriet, J.-P., the MiCROSYSTEMS MD 169 shipboard party, 2011. Cold-water coral mounds on the pen Duick escarpment, gulf of Cadiz: the MiCROSYSTEMS project approach. Mar. Geol. 282 (Issues 1–2), 102–117pp. https://doi.org/10.1016/j.margeo.2010.08.012.

Van Rooij, D., De Mol, B., Huvenne, V., Ivanov, M., Henriet, J.-P., 2003. Seismic evidence of current-controlled sedimentation in the Belgica mound province, upper Porcupine slope, southwest of Ireland. Mar. Geol. 195 (1–4), 31–53. https://doi.org/10.1016/S0025-3227(02)00681-3.

Vergés, J., Fernàndez, M., 2012. Tethys-Atlantic interaction along the Iberia-Africa plate boundary: the Betic-Rif orogenic system. Tectonophysics 579, 144–172. https://doi.org/10.1016/j.tecto.2012.08.032.

Wang, H., Lo Iacono, C., Wienberg, C., Titschack, J., Hebbeln, D., 2019. Cold-water coral mounds in the southern Alboran Sea (western Mediterranean Sea): internal waves as an important driver for mound formation since the last deglaciation. Mar. Geol. 412, 1–18. https://doi.org/10.1016/j.margeo.2019.02.007.

Wienberg, C., Titschack, J., Frank, N., De Pol-Holz, R., Fietzke, J., Eisele, M., Kremer, A., Hebbeln, D., 2020. Deglacial upslope shift of NE Atlantic intermediate waters controlled slope erosion and cold-water coral mound formation (Porcupine Seabight, Irish margin). Quat. Sci. Rev. 237, 106310 https://doi.org/10.1016/j.quascirev.2020.106310.

Wienberg, C., Titschack, J., Freiwald, A., Frank, N., Lundälv, T., Taviani, M., Beuck, L., Schröder-Ritzrau, A., Krengel, T., Hebbeln, D., 2018. The giant Mauritanian cold-water coral mound province: oxygen control on coral mound formation. Quat. Sci. Rev. 185, 135–152. https://doi.org/10.1016/j.quascirev.2018.02.012.

Wienberg, C., Frank, N., Mertens, K.N., Stuut, J.-B., Marchant, M., Fietzke, J., Mienis, F., Hebbeln, D., 2010. Glacial cold-water coral growth in the Gulf of Cádiz: implications of increased palaeo-productivity. Earth Planet Sci. Lett. 298, 405–416. https://doi.org/10.1016/j.epsl.2010.08.017.

Wienberg, C., Hebbeln, D., Fink, H.G., Mienis, F., Dorschel, B., Vertino, A., López Correa, M., Freiwald, A., 2009. Scleractinian cold-water corals in the Gulf of Cádiz – first clues about their spatial and temporal distribution. Deep Sea Res. Oceanogr. Res. Pap. 56 (10), 1873–1893. https://doi.org/10.1016/j.dsr.2009.05.016.

Xu, S., Menapace, W., Hüpers, A., Kopf, A., 2021. Mud volcanoes in the Gulf of Cadiz as a manifestation of tectonic processes and deep-seated fluid mobilization. Mar. Petrol. Geol. 132, 105188 https://doi.org/10.1016/j.marpetgeo.2021.105188.

Yin, S., Hernández-Molina, F.J., Zhang, W., Li, J., Wang, L., Ding, W., Ding, W., 2019. The influence of oceanographic processes on contourite features: a multidisciplinary study of the northern South China Sea. Mar. Geol. 415, 105967 https://doi.org/10.1016/j.margeo.2019.105967.

Zenk, W., Armi, L., 1990. The complex spreading pattern of Mediterranean Water off the Portuguese continental slope. Deep-Sea Res., Part A 37, 1805–1823. https://doi.org/10.1016/0198-0149(90)90079-B.

Zitellini, N., Gràcia, E., Matias, L., Terrinha, P., Abreu, M.A., De Alteriis, G., Henriet, J.P., Dañobeitia, J.J., Masson, D.G., Mulder, T., Ramella, R., Somoza, L., Diez, S., 2009. The quest for the Africa-Eurasia plate boundary west of the Strait of Gibraltar. Earth Planet Sci. Lett. 280, 13–50. https://doi.org/10.1016/j.epsl.2008.12.005.